The size of plume heterogeneities constrained by Marquesas isotopic stripes

Catherine Chauvel, René C. Maury, Sylvain Blais, Eric Lewin, Hervé Guillou, Gérard Guille, Philippe Rossi, Marc-André M-A Gutscher

Geochemistry Geophysics Geosystems G3

Article
Volume 13, Number 1
12 July 2012
Q07005, doi:10.1029/2012GC004123
ISSN: 1525-2027

Published by AGU and the Geochemical Society

The size of plume heterogeneities constrained by Marquesas isotopic stripes

Catherine Chauvel
ISTerre, UMR 5275, CNRS, Université Grenoble 1, BP 53, FR-38041 Grenoble CEDEX 09, France (catherine.chauvel@ujf-grenoble.fr)

René C. Maury
Domaines Océaniques, UMR 6538, Université de Brest, Université Européenne de Bretagne, CNRS, Institut Universitaire Européen de la Mer, Place N. Copernic, FR-29280 Plouzané, France

Sylvain Blais
Géosciences Rennes, UMR 6518, Université de Rennes 1, Université Européenne de Bretagne, CNRS, Campus de Beaulieu, Avenue du Général Leclerc, FR-35042 Rennes CEDEX, France

Eric Lewin
ISTerre, UMR 5275, CNRS, Université Grenoble 1, BP 53, FR-38041 Grenoble CEDEX 09, France

Hervé Guillou
UMR 8212, LSCE-IPSL/CEA-CNRS-UVSQ, Domaine du CNRS, 12 avenue de la Terrasse, FR-91198 Gif-sur-Yvette, France

Gérard Guille
Laboratoire de Géophysique, CEA-DASE, FR-91680 Bruyères-le-Chatel, France

Philippe Rossi
BRGM, SGN-CGF, 3 avenue Claude-Guillemin, BP 36009, FR-45060 Orléans CEDEX 2, France

Marc-André Gutscher
Domaines Océaniques, UMR 6538, Université de Brest, Université Européenne de Bretagne, CNRS, Institut Universitaire Européen de la Mer, Place N. Copernic, FR-29280 Plouzané, France

[1] The scale and geometry of chemical and isotopic heterogeneities in the source of plumes have important scientific implications on the nature, composition and origin of plumes and on the dynamics of mantle mixing over time. Here, we address these issues through the study of Marquesas Islands, one of the Archipelagoes in Polynesia. We present new Sr, Nd, Pb, Hf isotopes as well as trace element data on lavas from several Marquesas Islands and demonstrate that this archipelago consists of two adjacent and distinct rows of islands with significantly different isotopic compositions. For the entire 5.5 Ma construction period, the northern islands, hereafter called the *Ua Huka group*, has had systematically higher $^{87}Sr/^{86}Sr$ and lower $^{206}Pb/^{204}Pb$ ratios than the southern *Fatu Hiva group* at any given $^{143}Nd/^{144}Nd$ value. The shape and curvature of mixing arrays preclude the ambient depleted MORB mantle as one of the mixing end-members. We believe therefore that the entire isotopic heterogeneity originates in the plume itself. We suggest that the two Marquesas isotopic stripes originate from partial melting of two adjacent filaments contained in small plumes or "plumelets" that came from a large dome structure located deep in

the mantle under Polynesia. Low-degree partial melting under Marquesas and other "weak" Polynesian hot spot chains (Pitcairn-Gambier, Austral-Cook, Society) sample small areas of the dome and preserve source heterogeneities. In contrast, more productive hot spots build up large islands such as Big Island in Hawaii or Réunion Island, and the higher degrees of melting blur the isotopic variability of the plume source.

Components: 14,000 words, 12 figures, 3 tables.

Keywords: Marquesas; isotopes; ocean island; plume structure.

Index Terms: 1025 Geochemistry: Composition of the mantle; 1030 Geochemistry: Geochemical cycles (0330); 1040 Geochemistry: Radiogenic isotope geochemistry.

Received 23 February 2012; **Revised** 24 May 2012; **Accepted** 7 June 2012; **Published** 12 July 2012.

Chauvel, C., R. C. Maury, S. Blais, E. Lewin, H. Guillou, G. Guille, P. Rossi, and M.-A. Gutscher (2012), The size of plume heterogeneities constrained by Marquesas isotopic stripes, *Geochem. Geophys. Geosyst.*, *13*, Q07005, doi:10.1029/2012GC004123.

1. Introduction

[2] The considerable isotopic heterogeneity in plume-related basalts is attributed to processes such as (i) chemical heterogeneity of mantle plumes at depth [*Kerr et al.*, 1995], (ii) entrainment of surrounding asthenospheric mantle materials [*Hart et al.*, 1992] or (iii) plume-lithosphere interactions [*Saunders et al.*, 1992]. There is ongoing debate about the relative importance of the three processes in the genesis of basaltic magmas from Iceland [*Chauvel and Hémond*, 2000; *Fitton et al.*, 2003; *Thirlwall et al.*, 2004; *Kokfelt et al.*, 2006], the Galapagos [*White et al.*, 1993; *Hoernle et al.*, 2000; *Blichert-Toft and White*, 2001; *Saal et al.*, 2007], Afar [*Furman et al.*, 2006; *Beccaluva et al.*, 2009; *Daoud et al.*, 2010] and Hawaii [*Yang et al.*, 2003; *Frey et al.*, 2005; *Fekiacova et al.*, 2007]. In particular, differences in lead isotopes between the Kea and Loa trends in Hawaii have been attributed to a bilateral asymmetry of the plume [*Abouchami et al.*, 2005; *Farnetani and Hofmann*, 2009, 2010].

[3] Large isotopic variations in Marquesas basalts have been known for decades [*Vidal et al.*, 1984; *Duncan et al.*, 1986; *Dupuy et al.*, 1987; *Vidal et al.*, 1987; *Woodhead*, 1992; *Desonie et al.*, 1993; *Caroff et al.*, 1995; *Le Dez et al.*, 1996; *Castillo et al.*, 2007] and have been attributed to (i) a concentrically zoned structure of the Marquesas plume [*Duncan et al.*, 1986], (ii) small-scale heterogeneities within the plume [*Dupuy et al.*, 1987; *Vidal et al.*, 1987; *Le Dez et al.*, 1996] or (iii) plume-lithosphere interactions [*Duncan et al.*, 1986; *Woodhead*, 1992; *Desonie et al.*, 1993; *Caroff et al.*, 1995]. These models were primarily based on a limited set of samples collected during reconnaissance sampling in the early 1970s by R.A. Duncan, R. Brousse, H. Craig and H.G. Barsczus, and during a single dredging cruise on Marquesas seamounts [*Desonie et al.*, 1993]. All these studies focused on the origin of the isotopic diversity and they did not use recently developed high-precision isotopic analyses to investigate potential relationships with a plume track or changes in source compositions as a function of time or distance to the presumed location of the active plume.

[4] The Marquesas archipelago has also been the object of great interest for geophysical studies, particularly since McNutt and coworkers [*McNutt*, 1998; *McNutt and Bonneville*, 2000] discovered that French Polynesia was built on top of a large topographic height attributed to the so-called Polynesian Superswell. Its existence is usually thought to be linked to the presence of a large region of hot material rising from deep in the mantle [*Davaille*, 1999; *Romanowicz and Gung*, 2002; *Courtillot et al.*, 2003; *Montelli et al.*, 2006] but the way these observations relate to geochemical constraints remains unsolved.

[5] Here we reexamine the scale of isotopic variations using high-precision Sr, Nd, Hf and Pb isotopic measurements obtained on a large set of new samples that were collected and dated during the first detailed geological mapping of Marquesas Islands. We demonstrate the existence of isotopic stripes different from those suggested recently by *Huang et al.* [2011] and we propose that they originate from small-scale heterogeneities located within elongated filaments in rising plumelets

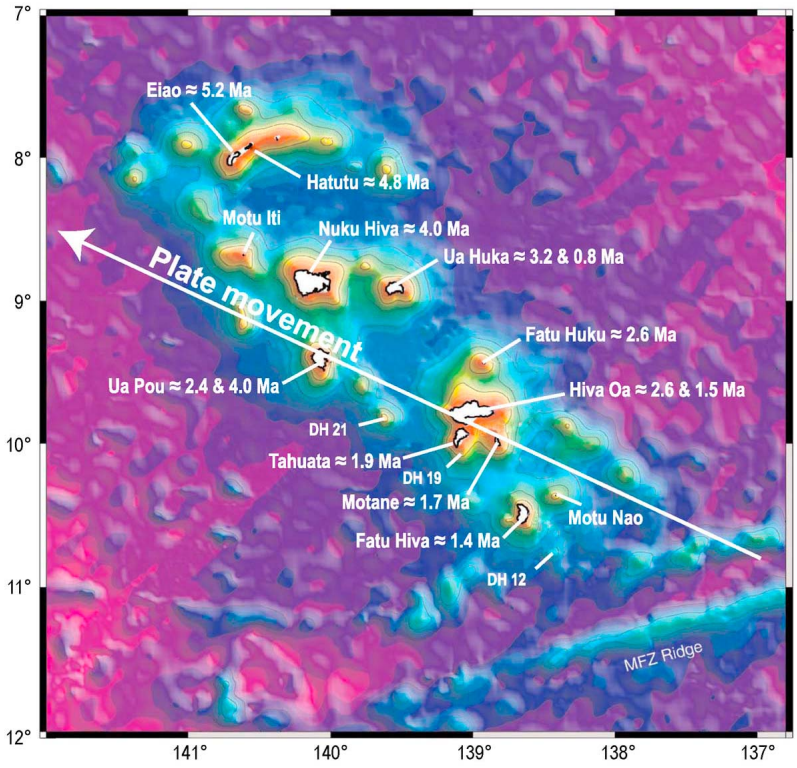

Figure 1. Location map of Marquesas Islands. The bathymetry comes from the global altimetry data set of *Smith and Sandwell* [1997]. Shades of purple denote depths of 5,000 to 4,000 m; shades of blue, depths of 4,000 to 2,000 m and shades of orange, depths less than 2,000 m. The main trend of the Marquesas chain is N40°W. Current Pacific plate motion is 10.5 cm/yr at N65°W, corresponding to the line shown in white and labeled plate movement. This line is also the line separating the two groups of islands as shown in Figures 4 and 5. In Hiva Oa, the line is located on the southwestern side of the island in the Taaoa Bay (see Figure S1 for more details). MFZ: Marquesas Fracture Zone.

coming from a large dome structure. Further comparison with other ocean islands suggests that weak plume-derived islands such as Polynesia are ideal sites to determine the scale of plume heterogeneities while strong plume-derived islands such as Hawaii are the best choices to establish the average composition of plumes.

2. Geological Setting of the Marquesas Archipelago

[6] The ca. 350 km-long Marquesas Archipelago is located in northern French Polynesia. It includes eight main islands (Eiao, Nuku Hiva, Ua Huka, Ua Pou, Hiva Oa, Tahuata, Motane, Fatu Hiva; Figure 1) and a few islets ("motus") and seamounts (Figure 1). Their age decreases toward the SE [*Duncan and McDougall*, 1974] from 5.5 Ma in Eiao to 0.6–0.35 Ma on a seamount south of Fatu Hiva (DH12 [*Desonie et al.*, 1993]). The Marquesas Islands lie on 53–49 Ma old oceanic crust generated at the axis of the Pacific-Farallon ridge. This crust is anomalously shallow given its age [*Crough and Jarrard*, 1981] and the so-called "Marquesas swell" has been interpreted as resulting from uplift due to a rising mantle plume [*Crough and Jarrard*, 1981]. However, the crustal thickness reaches 15–20 km below the central part of the Archipelago [*Filmer et al.*, 1993; *Caress et al.*, 1995], and the swell could also result from the buoyancy of such a thick basaltic crust [*McNutt and Bonneville*, 2000]. The origin of the crustal thickening was attributed either to (i) Plio-Quaternary underplating of plume magmas just below the Moho [*Caress et al.*, 1995; *McNutt and Bonneville*, 2000] or (ii) to the edification of the Archipelago over a small 50–45 Ma old oceanic plateau that formed near the axis of the Pacific-Farallon ridge [*Gutscher et al.*, 1999].

[7] The Marquesas Archipelago is atypical in many other respects [*Brousse et al.*, 1990; *Guille et al.*, 2002; *Devey and Haase*, 2003; *Legendre et al.*, 2006]. It is generally linear but its N30–40°W direction is slightly oblique to that of the Pacific plate movement (Figure 1). In contrast, it is parallel

to the spreading motion of the Pacific-Farallon ridge prior to the onset of accretion along the East Pacific Rise. This feature suggests that tectonic features and/or zones of weakness in the underlying Pacific-Farallon plate might have controlled the emplacement of the Plio-Quaternary Marquesas magmas [*Crough and Jarrard*, 1981; *McNutt et al.*, 1989; *Brousse et al.*, 1990].

[8] A final puzzling feature is that no active volcanoes are known at the southeastern end of the chain. ^{40}K-^{40}Ar ages younger than 1 Ma have only been obtained on a seamount south of Fatu Hiva (DH12, [*Desonie et al.*, 1993]), and on the post-shield strombolian Teepoepo and Tahoatikikau cones on Ua Huka (Table 1 and Table S1 in the auxiliary material).[1] Most authors consider that the Marquesas Fracture Zone (MFZ) [*Pautot and Dupont*, 1974] may have terminated the hot spot activity [*McNutt et al.*, 1989; *Brousse et al.*, 1990; *Guille et al.*, 2002]. However, the MFZ is aseismic [*Jordahl et al.*, 1995] and young volcanic rock has not been recovered from the adjacent Marquesas Fracture Zone Ridge (MFZ ridge; Figure 1). The seamount chain parallel to the MFZ ridge ca. 50 km to the north (Figure 1) has not yet been dredged and it could potentially be the present location of Marquesas hot spot activity.

[9] Most previous authors have used the main N30–40°W trend of the Marquesas Archipelago, oblique to the current N65°W motion of the Pacific plate, to draw age-distance plots and these display considerable scatter [*Brousse et al.*, 1990; *Desonie et al.*, 1993; *Guille et al.*, 2002]. Similar plots using the N65°W trend give better fits [*Legendre et al.*, 2006], especially when considering only unspiked ^{40}K-^{40}Ar ages measured on separated groundmass [*Charbit et al.*, 1998] because they are less scattered than conventional data on whole rocks.

[10] Marquesas basaltic lavas range from quartz tholeiites to basanites [*Guille et al.*, 2002]. Generally speaking, alkalinity tends to increase through time in a given island, e.g., Nuku Hiva or Ua Huka. Shields are often tholeiitic while post-shield lavas are often alkaline, but there are many exceptions. For instance, alkali basalts and basanites make up most of the shield of Ua Pou [*Legendre et al.*, 2005b]. Alkaline lavas also occur in the shields of Eiao [*Caroff et al.*, 1995], Motane and Tahuata [*Maury et al.*, 2012], and conversely tholeiites are present in the post-shield units of Nuku Hiva [*Legendre et al.*, 2005a], Hiva Oa, Fatu Hiva and Tahuata [*Maury et al.*, 2012].

[11] Here, we present new geochemical data obtained on five Marquesas Islands: Ua Huka, Fatu Hiva, Hiva Oa, Motane and Tahuata. The simplified geological maps shown in Figure S1 highlight their main features. The five islands have very different sizes with only 13 km^2 for Motane and about 320 km^2 for Hiva Oa. Motane represents the crescent-shaped remnant of the caldeira walls of a large shield volcano. Ua Huka, Tahuata and Fatu Hiva Islands consist in external shield volcanoes in the caldeira of which are nested post-shield inner volcanoes (Figure S1). There is usually little to no time gap between the end of edification of the shield and the start of the post-shield volcano for all these islands (Figure S1). Ua Huka shows, in addition, two much younger edifices attributed to a Quaternary rejuvenation of volcanism [*Legendre et al.*, 2006]. Finally, Hiva Oa consists of three coalescent shields, the central one being partly overlain by post-shield lavas (Figure S1).

3. Analytical Techniques

[12] Before chemical analyses, all samples were crushed using an agate mortar. Major element data were obtained by Inductively Coupled Plasma-Atomic Emission Spectrometry (ICP-AES) at IUEM, Plouzané using the method of *Cotten et al.* [1995]. The international standards used for calibration were ACE, BEN, JB-2, PM-S and WS-E and the relative standard deviations are ±1% for SiO_2, and ±2% for other major elements except P_2O_5 and MnO (absolute precision ±0.01%). Trace elements were measured on the same rock powders using an ICP-MS in Grenoble and the method described in detail by Chauvel *et al.* [2011]. Reproducibility of the measurements is typical better than 5% and the accuracy of the measured concentrations is better than 5%, as testified by repeated measurements of international rock standards (BHVO-2, BR, BEN, BR 24) (see Table S2).

[13] To avoid potential contamination of the samples during crushing, rock chips were used for the isotopic measurements. The chips were leached using 6N HCl for about one hour and the leachate was discarded. The leached chips were dissolved in ultra-clean HF combined with HNO_3. The chemical protocol is described by *Chauvel et al.* [2011] but we also specify that Pb was isolated using a two columns procedure to insure proper purification of the element. Several blanks were measured during the

[1]Auxiliary materials are available in the HTML. doi:10.1029/2012GC004123.

Table 1. Sr, Nd, Hf, and Pb Isotopic Compositions of Lavas From Ua Huka, Fatu Hiva, Hiva Oa, Motane, and Tahuata[a]

Sample	Volcano	Rock Type	Longitude	Latitude	Age (Ma)	$^{87}Sr/^{86}Sr$	$\pm2\sigma_m$	$^{87}Sr/^{86}Sr_{initial}$	$^{206}Pb/^{204}Pb$	$^{207}Pb/^{204}Pb$	$^{208}Pb/^{204}Pb$	$^{143}Nd/^{144}Nd$	$\pm2\sigma_m$	$^{176}Hf/^{177}Hf$	$\pm2\sigma_m$
						Ua Huka									
Shield-building phase															
UH27	Hikitau	Olivine tholeiite	−139.5024	−8.8998	3.11	0.705312	8	0.705303	19.138	15.609	39.086	0.512778	4	0.282938	5
UH27 Dup						0.705318	9	0.705309						0.282936	5
UH66	Hikitau	Olivine tholeiite	−139.5909	−8.8873	3.11	0.705274	9	0.705265	19.160	15.614	39.130	0.512769	13	0.282942	6
UH98	Hikitau	Olivine tholeiite	−139.6011	−8.9325	2.94	0.705330	10	0.705322	19.205	15.620	39.165	0.512814	14	0.282925	5
Post shield phase															
UH81	Hane	Alkali basalt	−139.5305	−8.924	2.97	0.705846	9	0.705837	19.188	15.628	39.195	0.512761	18	0.282899	4
UH89	Hane	Alkali basalt	−139.5456	−8.9312	2.43	0.705840	9	0.705838	19.137	15.624	39.182	0.512733	15	0.282890	4
UH93	Hane	Alkali basalt	−139.5744	−8.9228	2.83	0.705496	9	0.705488	19.099	15.618	39.138	0.512752	14	0.282927	5
UH97	Hane	Alkali basalt	−139.5885	−8.9251	2.70	0.704679	7	0.704673	19.315	15.623	39.270	0.512847	15	0.282932	4
UH97 Dup						0.704656	7	0.704650							
UH47	Hane	Trachyte	−139.5299	−8.9354	2.93	0.706352	33	0.706076	19.138	15.625	39.194	0.512710	11	0.282882	5
UH47 Dup														0.282883	4
UH53	Hane	Phonolite	−139.5625	−8.9022	2.71	0.705819	10	0.705575	18.965	15.591	38.935	0.512806	11	0.282981	4
UH71	Hane	Trachyte	−139.6105	−8.9241	2.92	0.706469	6	0.706085	19.128	15.624	39.180	0.512719	15	0.282886	4
Rejuvenated volcanism															
UH34	Tahoatikikau	Basanite	−139.5705	−8.9287	0.763	0.704440	8	0.704438	18.898	15.560	38.844	0.512901	15	0.283039	4
UH34 Dup						0.704426	7	0.704424	18.897	15.557	38.834				
UH65	Tahoatikikau	Basanite	−139.5628	−8.9358	0.822	0.704487	8	0.704487	18.830	15.551	38.769	0.512860	14	0.283058	4
UH40	Tahoatikikau	Basanite	−139.5696	−8.9203	0.785	0.704517	7	0.704515	19.064	15.587	39.079	0.512842	14	0.283012	4
UH50	Teepoepo	Basanite	−139.5709	−8.9187	0.963	0.704397	6	0.704394	18.991	15.565	38.909	0.512861	14	0.283024	5
UH35	Teepoepo	Basanite	−139.5613	−8.9394	1.150	0.704264	9	0.704262	18.918	15.563	38.821	0.512882	13	0.283037	5
UH62	Teepoepo	Basanite	−139.5881	−8.9366	1.030	0.704447	11	0.704446	18.897	15.560	38.822	0.512894	16	0.283037	6
						Fatu Hiva									
Shield-building phase															
FH13	Touaouho	Olivine tholeiite	−138.6185	−10.4844	1.81	0.704349	3	0.704346	19.308	15.613	39.126	0.512839	9	0.283020	22
FH17	Touaouho	Olivine tholeiite	−138.6503	−10.4326	1.49	0.703644	3	0.703641	19.656	15.619	39.391	0.512893	6	0.283015	8
FH18	Touaouho	Olivine tholeiite	−138.6811	−10.4227	1.35	0.703711	3	0.703709	19.626	15.624	39.352	0.512878	8	0.282976	8
Post shield phase															
FH01	Omoa	Olivine tholeiite	−138.6598	−10.4773	1.37	0.703589	3	0.703587	19.688	15.619	39.415	0.512874	7	0.282982	15
FH11	Omoa	Olivine tholeiite	−138.6587	−10.4688	1.26	0.704110	3	0.704108	19.393	15.621	39.145	0.512842	7	0.282977	5
						Hiva Oa									
Shield-building phase															
HV64	Taaoa	Olivine tholeiite	−139.1466	−9.8368	2.55	0.703516	3	0.703513	19.524	15.604	39.257	0.512914	7	0.283001	5
HV76	Temetiu	Olivine tholeiite	−139.0605	−9.7620	2.02	0.705139	3	0.705134	19.054	15.613	38.968	0.512788	9	0.282933	6
HV76 Dup												0.512790	7	0.282929	8

Table 1. (continued)

Sample	Volcano	Rock Type	Longitude	Latitude	Age (Ma)	$^{87}Sr/^{86}Sr$	$\pm 2\sigma_m$	$^{87}Sr/^{86}Sr_{initial}$	$^{206}Pb/^{204}Pb$	$^{207}Pb/^{204}Pb$	$^{208}Pb/^{204}Pb$	$^{143}Nd/^{144}Nd$	$\pm 2\sigma_m$	$^{176}Hf/^{177}Hf$	$\pm 2\sigma_m$
Motane															
Shield-building phase															
MT04		Olivine tholeiite	−138.8341	−9.9599	1.59	0.703111	3	0.703110	19.725	15.595	39.365	0.512972	6	0.283031	8
MT04 Dup						0.703091	3	0.703090	19.724	15.592	39.363				
MT08		Olivine tholeiite	−138.8305	−9.9625	1.53	0.703953	3	0.703950	19.460	15.614	39.184	0.512886	10	0.283015	12
MT12		Basanite	−138.8021	−10.0199	1.96	0.704686	4	0.704682				0.512797	9	0.282984	7
MT12 Dup												0.512800	7	0.282969	6
Tahuata															
Shield-building phase															
TH04	Vaitapu	Alkali basalt	−139.0555	−9.9107	1.80	0.705114	3	0.705109				0.512755	6	0.282888	17
TH05	Vaitapu	Basanite	−139.0903	−9.8927	1.80	0.705154	3	0.705150	19.137	15.615	39.106	0.512742	7	0.282926	8
TH13	Vaitapu	Quartz tholeiite	−139.1118	−9.9776	1.88	0.703455	3	0.703454	19.495	15.602	39.315	0.512913	6	0.282999	9
TH14	Vaitapu	Alkali basalt	−139.0802	−9.9158	1.80	0.705550	3	0.705549	19.112	15.624	39.165	0.512723	11	0.282872	11
TH18	Vaitapu	Olivine tholeiite	−139.099	−9.9267	1.82	0.704608	3	0.704603	19.215	15.615	39.186	0.512804	9	0.282946	8
TH39	Vaitapu	Olivine tholeiite	−139.1252	−9.9756	2.11	0.704353	3	0.704348	19.305	15.607	39.227	0.512838	7	0.282963	16
Post shield phase															
TH08	Hanatetena	Hawaiite	−139.0833	−9.9629	1.74	0.704777	3	0.704772	19.112	15.610	39.051	0.512814	7	0.282964	8
TH31	Hanatetena	Quartz tholeiite	−139.1069	−9.9866	1.80	0.703902	3	0.703901	19.440	15.610	39.329	0.512853	6	0.282986	13

[a]The average daily measurements of the Ames-Grenoble Hf standard ranged from 0.282153 to 0.282162 (23 measurements) and all data are normalized to 0.282160, the value recommended by *Chauvel et al.* [2011]. The average daily measurements for the Ames-Rennes Nd standard ranged from 0.511967 to 0.511980 (29 measurements) and all data are normalized to 0.511961, the value recommended by *Chauvel and Blichert-Toft* [2001]. The average $^{87}Sr/^{86}Sr$ value for the NBS 987 standard was 0.710263 (9 measurements). Based on repeated measurements of NBS 981, we estimate maximum errors on the Pb isotopic ratios at 100 ppm for $^{206}Pb/^{204}Pb$, 150 ppm for $^{207}Pb/^{204}Pb$ and 200 ppm for $^{208}Pb/^{204}Pb$. Sources of ages: unspiked ^{40}K-^{40}Ar ages measured on separated groundmass and reported in Table S1 and in *Blais et al.* [2008] for Ua Huka. Based on field relationships, the age of UH66 is assumed to be similar to that of UH27, the age of MT12 similar to that of MT11 and the ages of TH04 and TH05 similar to that of TH14. Longitudes and latitudes are expressed in decimal degrees. The $^{87}Sr/^{86}Sr$ initial ratios were calculated using the Rb and Sr concentrations reported in Table S2. Dup stands for complete duplicate analysis.

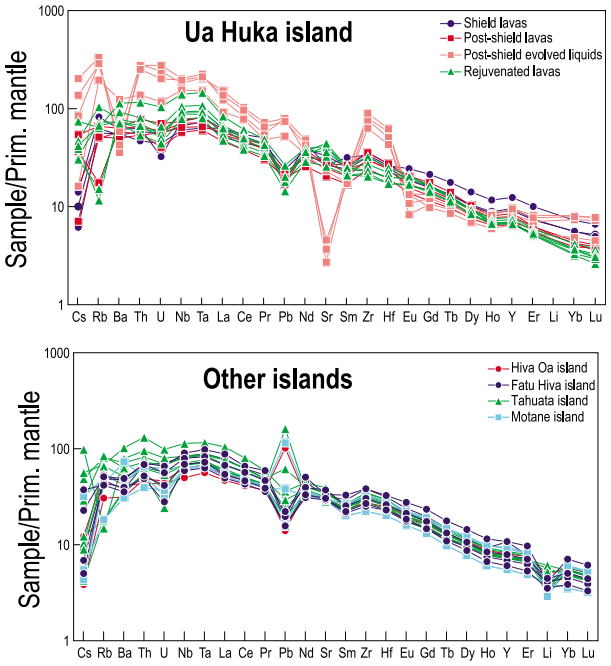

Figure 2. Incompatible trace element patterns of Marquesas samples. Samples from Ua Huka are grouped as shield, post-shield and rejuvenated while no distinction is made for samples from Hiva Oa, Fatu Hiva, Tahuata and Motane. Primitive mantle values are from *McDonough and Sun* [1995].

course of the study. They were lower than 70 picograms for Pb, 50 picograms for Sr, 40 picograms for Nd and 40 picograms for Hf. These values are all insignificant relative to the amount of element isolated for each isotopic system.

[14] Hf and Nd isotopic measurements were performed at ENS Lyon using the Nu instrument, normalizing ratios $^{179}Hf/^{177}Hf = 0.7325$ and $^{146}Nd/^{144}Nd = 0.7219$, and a daily bias correction based on the average measurement of Ames-Grenoble Hf and Ames-Rennes Nd standards (see footnote of Table 1). The same instrument was used for the Pb isotopes. Mass fractionation was corrected using the Tl addition technique [*White et al.*, 2000] and standard bracketing with the NBS 981 standard which was measured every third sample. Standard values are from *Galer and Abouchami* [1998]. Sr isotopic ratios were measured on a TIMS in Brest in static mode. Values measured for the NBS 987 standard during the course of the study are given in the footnote of Table 1.

[15] K-Ar ages were obtained at LSCE (Laboratoire des Sciences du Climat et de l'environnement) in Gif-sur-Yvette. The samples were crushed, sieved to 0.25–0.125 mm size fraction and ultrasonically washed in acetic acid. Potassium and argon were measured on the microcrystalline groundmass, after removal of phenocrysts using heavy liquids and magnetic separations. This process removes at least some potential sources of systematic error due to the presence of excess ^{40}Ar in olivine and feldspar phenocrysts [*Laughlin et al.*, 1994]. The K content of the separated groundmass was measured by ICP-AES in Brest using the same method as for major elements while Ar analyses were performed in Gif-sur-Yvette using the procedures of *Guillou et al.* [2011]. Ages given in Table S1 were calculated using the constants recommended by *Steiger and Jäger* [1977].

4. Results

[16] Major and trace element data are provided in Table S2. Basalts belonging to the shield and post-shield phases are either tholeiitic or alkalic with SiO_2 contents ranging from 45 to 48% and MgO between 4 and 12%. In contrast, the rejuvenated phase of volcanic activity in Ua Huka consists of basanites with much lower SiO_2 (41–45%) and generally higher MgO contents. In Ua Huka, four differentiated rocks belonging to the post-shield phase were also analyzed. Trace elements for all samples are plotted as spidergrams in Figure 2. All basaltic lavas display patterns enriched in incompatible elements as usually observed in other ocean islands and no marked differences exist between the various islands. However, four samples (TH04 and TH13 from Tahuata, MT04 from Motane and HV76 from Hiva Oa) display positive Pb anomalies, a feature that might be explained by the presence of post-magmatic sulfides that occur sporadically in basaltic samples from these islands [*Maury et al.*, 2012]. In Ua Huka, the benmoreite, the two trachytes and the phonolite present very distinct trace element patterns (Figure 2) due to the effect of intense fractional crystallization.

[17] The new isotopic data obtained on five different Marquesas Islands are given in Table 1 and compared with published Nd, Sr, Hf and Pb isotopic ratios in Figure 3. Data from the five analyzed islands cover the entire range of known isotopic variation for the Marquesas in $^{87}Sr/^{86}Sr$ versus $^{143}Nd/^{144}Nd$ space: inclusion of samples from the shield-building phase of Ua Huka extend it to lower Nd and higher Sr (Figure 3a). In addition, each individual island defines a large field covering at least half of the total Marquesas variation. In comparison to Nd and Sr, Pb isotopic ratios are relatively constant (see Figures 3b and 3d) with $^{206}Pb/^{204}Pb$ ratios ranging only from 18.8 to 19.7

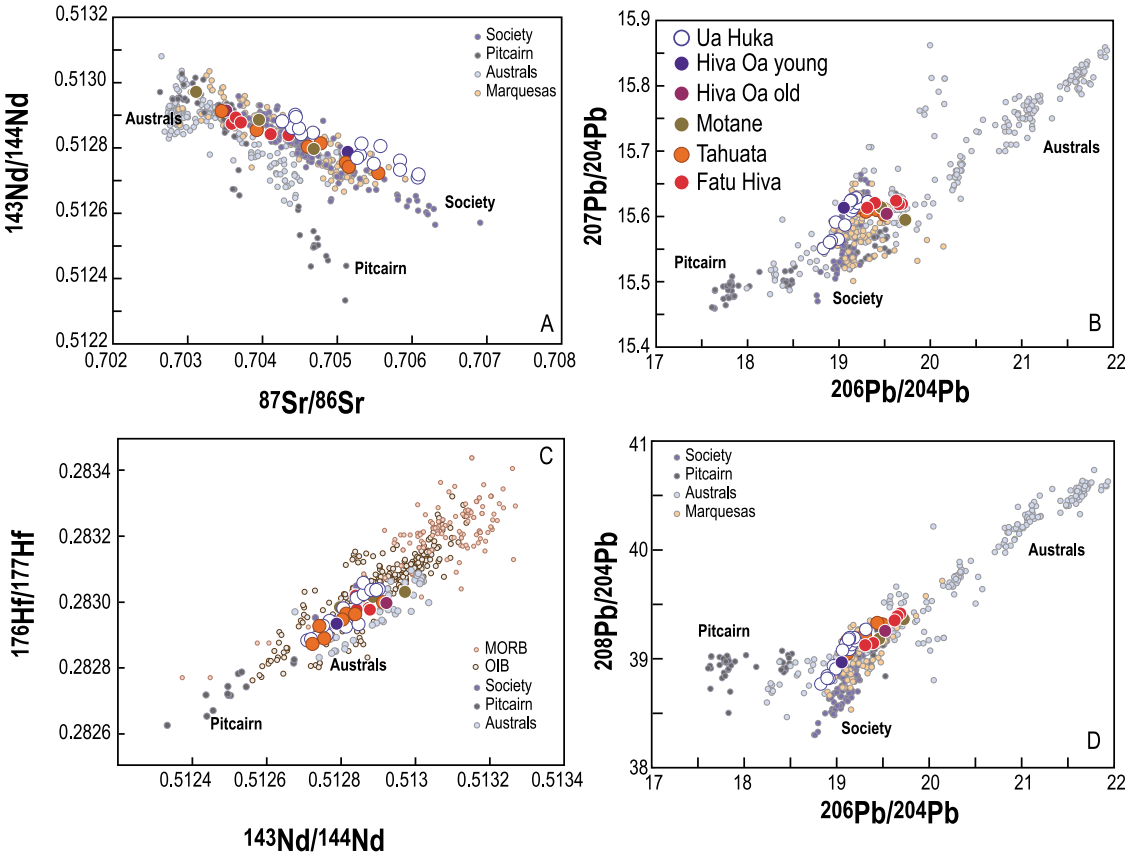

Figure 3. (a–d) Nd, Sr, Hf and Pb isotopic compositions of the Marquesas Islands. Data obtained on lavas from Ua Huka, Fatu Hiva, Hiva Oa, Motane and Tahuata are compared to data already published on the Marquesas [*Vidal et al.*, 1984; *Duncan et al.*, 1986; *Dupuy et al.*, 1987; *Vidal et al.*, 1987; *Woodhead*, 1992; *Desonie et al.*, 1993; *Caroff et al.*, 1995; *Cotten et al.*, 1995; *Le Dez et al.*, 1996; *Legendre et al.*, 2005a, 2005b; *Castillo et al.*, 2007], on other Polynesian Archipelagoes (GEOROC database) and to data reported for MORB and OIB in Figure 3c (GEOROC and PetDB databases). In Figure 3a, the initial Sr isotopic compositions are used because an age correction is necessary for few samples due to their elevated Rb/Sr ratio.

and $^{207}Pb/^{204}Pb$ from 15.55 to 15.63. The Hf isotopic compositions, the first reported for Marquesas Islands, vary between 0.28288 and 0.28306, correlate with Nd isotopic ratios, and define in Hf-Nd isotopic space an array located above the Austral-Cook Islands in the middle of the oceanic island array (see Figure 3c).

[18] The most interesting feature displayed by the isotopic data is the existence within the Marquesas Archipelago of two parallel arrays in Nd versus Sr isotopic space (Figure 4). Two groups of islands can be distinguished, one to the north, the other to the south of a N65°W line that follows the direction of the Pacific plate motion (see Figure 1) and passes through Hiva Oa where it separates the Taaoa shield from the other volcanoes (see map shown in Figure S1). The northern group of islands, shown by various shades of blue dots in Figure 4, includes Eiao, Hatutu, Nuku Hiva, Ua Huka, Fatu Huku and the young lavas from the eastern side of Hiva Oa Island (Puamau, Ootua and Temetiu volcanoes). The southern group, shown by various shades of orange dots in Figure 4, includes Ua Pou, Tahuata, the old Hiva Oa lavas (from the Taaoa volcano located on the western side of the island), Motane, Fatu Hiva and Motu Nao. Like *Chauvel et al.* [1997] who used the name of the youngest island for each of the three trends recognized along the Austral-Cook Island chain, we call the northern group the "*Ua Huka group*" and the southern group the "*Fatu Hiva group.*" The distinction between the two groups is not related to the age of the islands: volcanism in the *Ua Huka group* occurs over a time period from 5.52 Ma at Eiao to 0.76 Ma at Ua Huka (Table 2) while it extends from 4.0 Ma at Ua Pou to 0.35 Ma (seamount DH12 south of Fatu Hiva) in the *Fatu Hiva group.*

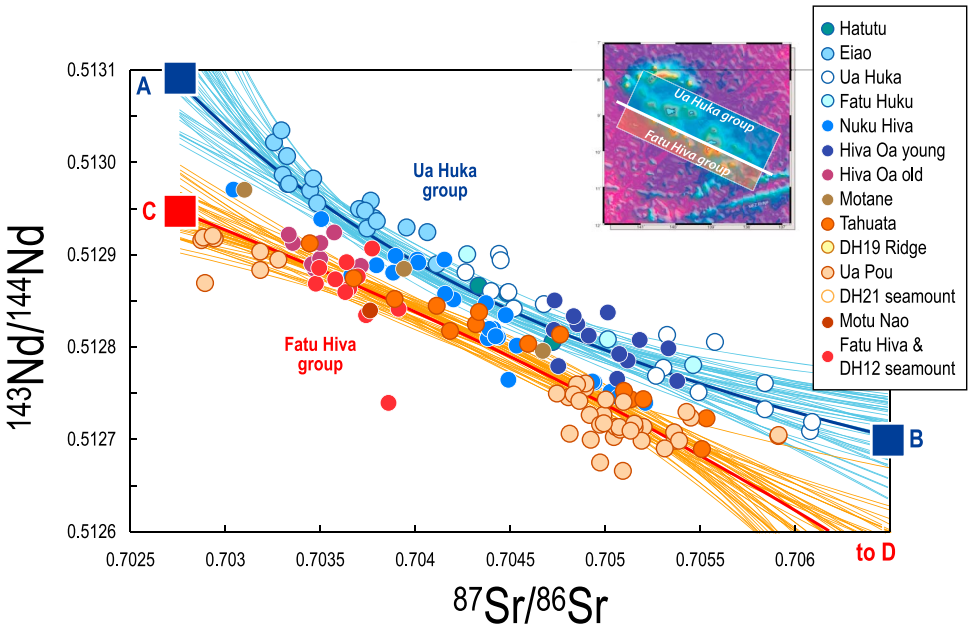

Figure 4. $^{87}Sr/^{86}Sr$ versus $^{143}Nd/^{144}Nd$ diagram showing the two parallel isotopic trends: the northern *Ua Huka trend* (blue) and the southern *Fatu Hiva trend* (red). Best fit regression curves are shown for each group (thick dark blue and red curves) as well as other regression curves corresponding to 2 sigma errors on the best regression (thin light blue and orange). The best fits for the *Ua Huka group* (blue symbols) and for the *Fatu Hiva group* (red symbols) constrain the $^{143}Nd/^{144}Nd$ of the depleted and enriched end-members (A and B for the *Ua Huka group* and C and D for the *Fatu Hiva group*) as well as the R values (values listed in Table 3). Data from this study and GEOROC database.

[19] Both groups define a very large range of isotopic compositions (for example, $^{87}Sr/^{86}Sr$ varies from 0.703 to 0.706 in the two groups) but the *Ua Huka group* has systematically higher Nd isotopic compositions at any given Sr isotopic composition. The distinction between the two groups is less clear in other isotopic spaces but in general the *Fatu Hiva group* has higher $^{206}Pb/^{204}Pb$ ratios than the *Ua Huka group* at any given $^{87}Sr/^{86}Sr$ or $^{143}Nd/^{144}Nd$ (Figures 5a and 5b). Finally, the

Table 2. Main Characteristics (Volume, Age, and Location) of the Marquesas Islands[a]

Island	Emerged Surface (km^2)	Edifice Volume (km^3)	Groundmass/Whole Rock K-Ar Ages		Distance to the MFZR Along N65W Trend (km)
			Max. (Ma)	Min. (Ma)	
Hatutu	6.5	9800	*4.90*	*4.70*	690
Eiao	44		5.52	4.95	680
Motu Iti	0.2	2900			580
Nuku Hiva	339	6950	4.53	3.62	525
Ua Huka	83	3250	3.24	0.76	480
Ua Pou	105	3250	4.00	2.35	440
Fatu Huku	1.3	6900	*2.65*	*2.54*	370
Hiva Oa	320		2.55	1.44	330
Tahuata	69	3850	2.11	1.74	310
Motane	13		1.96	1.53	280
Fatu Hiva	84	2800	1.81	1.11	175

[a]Submerged edifice volumes above the −3,000 m isobaths were calculated with the GMT software and emerged volumes from topographic maps. The corresponding total volume of volcanic edifices is estimated at 42,500 km^3. This value includes 2,800 km^3 of seamounts scattered throughout the archipelago (Figure 1). When available, unspiked ^{40}K-^{40}Ar ages measured on separated groundmass [*Charbit et al.*, 1998] were preferred to conventional data on whole rocks (Hatutu and Fatu Huku from *Brousse et al.* [1990] shown in italics) because of possible excess of radiogenic Ar into olivine and pyroxene phenocrysts [*Laughlin et al.*, 1994]. Sources of unspiked ages on groundmass: Table S1; *Caroff et al.* [1995] for Eiao; *Maury et al.* [2006] for Nuku Hiva; *Legendre et al.* [2006] and *Blais et al.* [2008] for Ua Huka; *Legendre et al.* [2005b] for Ua Pou and *Maury et al.* [2012] for Hiva Oa, Tahuata, Motane and Fatu Hiva. Two distinct volcanic events are recognized in Ua Huka (3.24–2.43 Ma and 1.15–0.76 Ma). Ages younger than 1 Ma only occur for Ua Huka and a seamount south of Fatu Hiva (DH12, 0.60–0.35 Ma [*Desonie et al.*, 1993]). MFZR: Marquesas Fracture Zone Ridge.

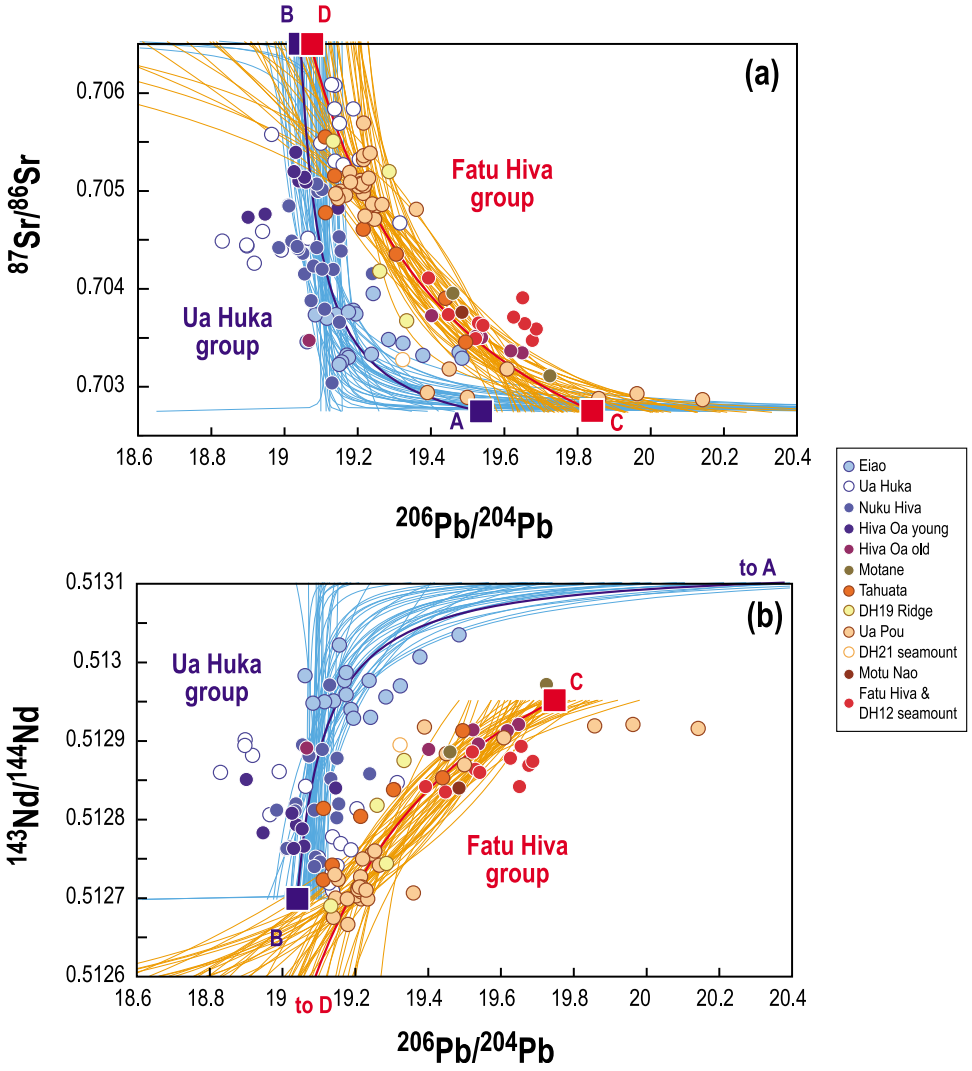

Figure 5. (a) $^{87}Sr/^{86}Sr$ and (b) $^{143}Nd/^{144}Nd$ versus $^{206}Pb/^{204}Pb$ for the Marquesas Islands. Best fit regressions are shown for each island group using the same symbols as in Figure 4. For the *Ua Huka group* (blue symbols), the $^{206}Pb/^{204}Pb$ of the depleted end-member (indicated by A) is poorly constrained using both Sr isotopes (Figure 5a) and Nd isotopes (Figure 5b) (values listed in Table 3); the *Ua Huka* enriched end-member (indicated by B) has a better constrained $^{206}Pb/^{204}Pb$ ratio using both Sr and Nd isotopes (values listed in Table 3); finally, the two R values are poorly constrained at about 20 (values listed in Table 3). For the *Fatu Hiva group* (red symbols), the $^{206}Pb/^{204}Pb$ of the depleted and enriched end-members (indicated by C and D) are better constrained (values listed in Table 3); it is also the case for the two R values (values listed in Table 3). Data from this study and GEOROC database.

maximum width on the seafloor of the *Ua Huka group* is about 120 km while that of the Fatu Hiva group is smaller at about 60 km (Figure 1).

5. Discussion

5.1. Is There a Relationship Between Timing of Eruptions, Types of Lavas and Isotopic Compositions?

[20] In some oceanic islands, a clear relationship exists between timing of lava eruption and chemical and isotopic compositions. For example, in Hawaii, extensive studies [e.g., *Garcia et al.*, 2010; *Hanano et al.*, 2010] demonstrated that the shield volcanic phase consists almost exclusively of tholeiites whose Sr isotopic compositions are systematically more radiogenic than those of the post-shield alkali lavas. In contrast, in Kerguelen, the opposite is observed [*Doucet et al.*, 2002]. In the Marquesas, no clear relationship exists. For example, in Ua Huka, the shield-building phase consists of tholeiites with radiogenic Sr isotopes associated with low Nd isotopic ratios and it is followed by an

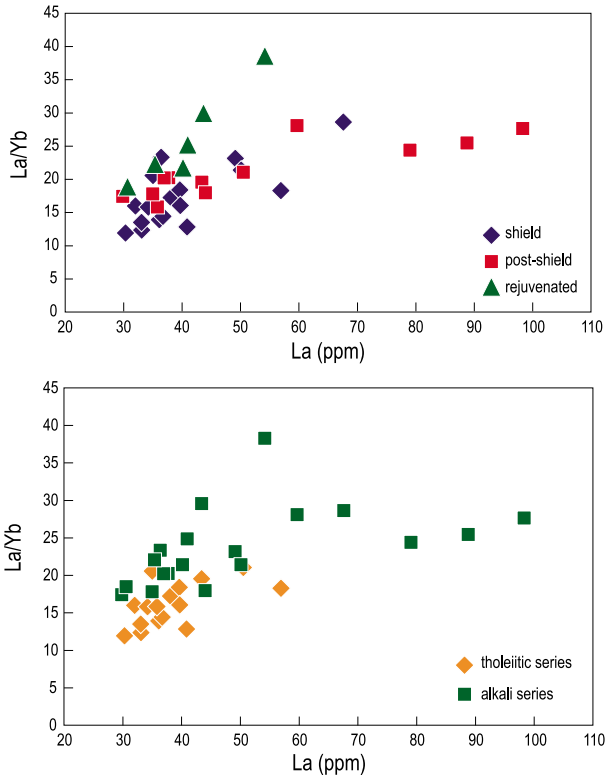

Figure 6. La/Yb versus La diagram for all new measurements on Marquesas lavas. No clear distinction exists between shield and post-shield lavas. In contrast, tholeiites and alkali basalts define two distinct fields. Data from Table S2.

alkaline post-shield phase with similar isotopic compositions (see Table 1). It is only the rejuvenated basanitic volcanism that has distinctly lower Sr isotopic compositions. In Tahuata and Motane, tholeiites and alkali basalts occur both in shield and post-shield phases (Table 1) while in Fatu Hiva and Hiva Oa only tholeiites exist. However, in all these islands, large Sr isotopic variability is observed. Our new results together with previously published data show therefore that no clear systematic exists and they do not support the claim that Marquesas shield lavas have lower $^{87}Sr/^{86}Sr$ ratios than post-shield lavas [*Castillo et al.*, 2007]. Our new trace element data also show that fractionation between highly incompatible and mildly incompatible trace elements is primarily controlled by degree of partial melting. Figure 6 clearly shows that when La/Yb is plotted as a function of La concentration, the alkali series defines a field with systematically higher La/Yb than the tholeiites, as expected if alkali basalts result from lower degrees of partial melting than tholeiites. In contrast, if the lavas are sorted as shield versus post-shield, no clear distinction exists and the only lavas with clearly higher La/Yb ratios are the basanites forming the Ua Huka rejuvenated volcanic phase. Finally, simple relationships between trace elements and isotopic compositions are not really obvious. *Willbold and Stracke* [2006], who compiled worldwide data for ocean island basalts, showed that the Ce/Pb ratio of EM-type lavas is usually lower than the canonical "mantle" value of 25 [*Hofmann et al.*, 1986] and that their Nb/U ratio is generally scattered and not significantly different from the value of 47 suggested by *Hofmann et al.* [1986]. They also mention that EM basalts have elevated Th/U ratios and lower Nb/Th ratios than HIMU basalts. Using our new data, we examine the relationship between these key trace element ratios and $^{87}Sr/^{86}Sr$, a good proxy for the intensity of the EM signal present in the various lavas. When taken as a whole, our new data define a scattered field for Ce/Pb versus $^{87}Sr/^{86}Sr$, but if samples with positive Pb anomalies (see Figure 2) are ignored, lavas define a broad negative trend between Ce/Pb ≈ 40 at low $^{87}Sr/^{86}Sr$ and Ce/Pb ≈ 20 at high $^{87}Sr/^{86}Sr$, covering the entire range reported for ocean island basalts (Figure 7). No clear relationship appears between $^{87}Sr/^{86}Sr$ and Nb/U or Th/U (Figure 7), but our data confirm the high Th/U suggested by *Willbold and Stracke* [2006], with an average value of 4.8. In contrast, when Nb/Th is plotted as a function of $^{87}Sr/^{86}Sr$ (Figure 7), a distinct negative trend is observed between Nb/Th ≈ 13 at low $^{87}Sr/^{86}Sr$ and Nb/Th ≈ 8 at high $^{87}Sr/^{86}Sr$; this relationship confirms the presence in the Marquesas plume source of low Nb sedimentary material as already suggested by numerous authors [*Dupuy et al.*, 1987; *Dostal et al.*, 1998; *Willbold and Stracke*, 2006]. In summary, the relationships between isotopic compositions as exemplified with $^{87}Sr/^{86}Sr$, and trace element ratios do not provide new and unambiguous constraints on the composition of the depleted and enriched end-members present in the source of Marquesas basalts but they confirm previous interpretations about the presence of crustal material in the source of lavas with elevated Sr isotopic compositions.

5.2. What Do the Isotopic Stripes Tell Us About the Plume Source?

[21] The origin of isotopic heterogeneities in ocean island basalts has focused scientific debate for decades [*Hart*, 1988], but only recently, with the appearance of high-precision Pb isotopic analyses, has fine isotopic structure been documented along ocean island chains. *Abouchami et al.* [2005] considered the two distinct Pb isotopic stripes first recognized in the pioneer work of *Tatsumoto*

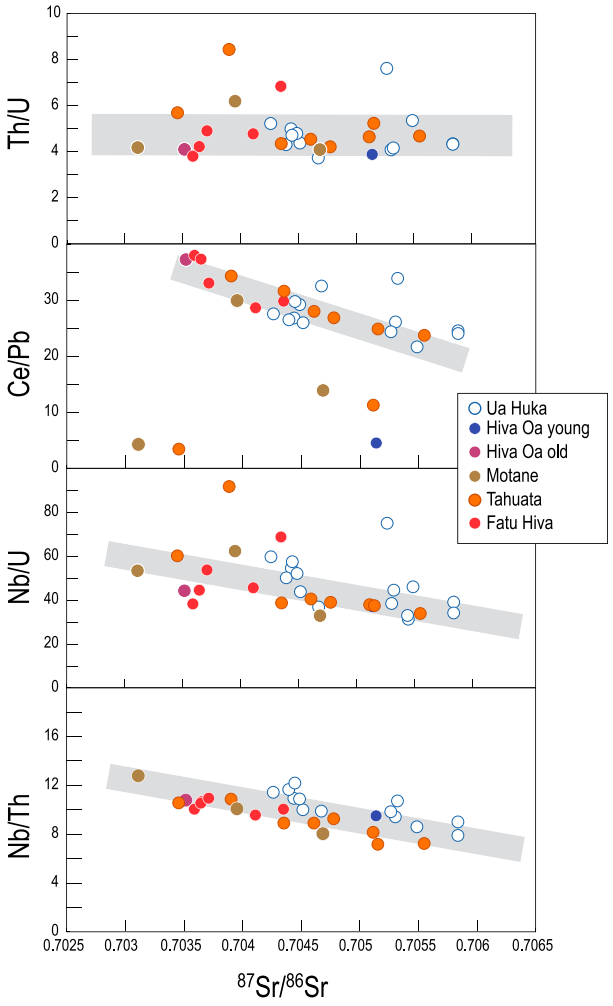

Figure 7. Th/U, Ce/Pb, Nb/U and Nb/Th ratios versus $^{87}Sr/^{86}Sr$ diagrams. We only plotted basalts from Table S2 and Table 1 and avoided the evolved liquids from Ua Huka because their trace element ratios differ probably from those of their source. Th/U is constant through the entire isotopic range with an average value of 4.8. If we exclude outliers, Ce/Pb, Nb/U and Nb/Th decrease when $^{87}Sr/^{86}Sr$ changes from 0.703 to 0.706.

[1978] for the Hawaiian plume as indicating its bilateral asymmetry. This interpretation led to heated debate about their origin and the shape of the heterogeneities within the mantle plume [*Abouchami et al.*, 2005; *Blichert-Toft and Albarède*, 2009; *Farnetani and Hofmann*, 2009, 2010]. Similar structures have now been observed in other ocean island basalts [*Chauvel et al.*, 2009; *Huang et al.*, 2011] and for other isotopic systems [*Weis*, 2010; *Weis et al.*, 2011] showing that they are more prevalent than previously thought.

[22] In Figure 4 we show that the relationship between Sr and Nd isotopic compositions in Marquesas lavas defines two parallel isotopic bands that are related to the position of the islands along the chain. The data previously published and compiled in the GEOROC database gave a hint [*Chauvel et al.*, 2009; *Huang et al.*, 2011] but our new data on Ua Huka, Hiva Oa, Tahuata, Fatu Hiva and Motane make the distinction extremely clear. The most striking feature comes from data for Hiva Oa where we observe that the 2.55 Ma old Taaoa volcano lavas, which are located on the western side of the island, belong to the *Fatu Hiva group* while the younger lavas (2.27 to 1.44 Ma) have very different isotopic compositions and belong clearly to the *Ua Huka group* (see Figure 4 and Tables S1 and S3 for high-precision ages and chemical compositions). The clear difference between the two groups within Hiva Oa shows that different mantle sources are sampled at distances less than 10 km and with a time difference of only 0.3 Ma (Table 1 and Figure S1).

[23] The difference between the two isotopic stripes observed along the Marquesas Archipelago can be evaluated in a quantitative way by calculating the statistical difference between the two arrays. The thick blue and red curves shown in Figure 4 represent the best fit to the fields defined by samples in each group. The only assumptions used to calculate the regression curves are the Sr isotopic compositions, which were fixed at 0.70275 and 0.70650 for the depleted and enriched end-members. In Figure 4, we show the two calculated regressions curves (thick dark blue and red curves) as well as the associated errors shown as thin blue and orange curves (see Text S1 for more explanations). The *Ua Huka group* defines an array between two end-members: a depleted one (A) with a $^{143}Nd/^{144}Nd$ ratio of 0.51311 ± 13 at $^{87}Sr/^{86}Sr = 0.70275$ and an enriched end-member (B) with a $^{143}Nd/^{144}Nd$ ratio of 0.51270 ± 6 at $^{87}Sr/^{86}Sr = 0.7065$. The mixing hyperbola has a curvature controlled by the ratio R of Sr/Nd in component A over Sr/Nd in component B of 2.2 (max: 5.7, min: 0.88) (see Table 3). In contrast the *Fatu Hiva group* defines a regression curve between a depleted end-member (C) with a $^{143}Nd/^{144}Nd$ ratio of 0.51295 ± 5 at $^{87}Sr/^{86}Sr = 0.70275$ and an enriched end-member (D) with a $^{143}Nd/^{144}Nd$ ratio of 0.51253 ± 18 at $^{87}Sr/^{86}Sr = 0.7065$ (see Figure 4 and Table 3). Here, the R ratio is equal to 0.73 (2.0, 0.27). Statistically, the two arrays have curvatures that are close to straight lines but the mixing end-members are significantly different.

[24] In isotopic spaces other than Sr versus Nd, the distinction between the two groups is less clear. Our new Hf isotopic data do not show a clear distinction between the two groups when combined

Table 3. Calculated Compositions for the Four Mixing End-Members

	Ua Huka Group		Fatu Hiva Group	
	Depleted Component A	Enriched Component B	Depleted Component C	Enriched Component D
$^{87}Sr/^{86}Sr$ (set)	0.70275	0.70650	0.70275	0.70650
$^{143}Nd/^{144}Nd$	0.51311 ± 13	0.51270 ± 6	0.51295 ± 5	0.51253 ± 18
$(Sr/Nd_{depl})/(Sr/Nd_{enrich})$	2.2 (max 5.7; min 0.88)		0.73 (max 2.0; min 0.27)	
$^{206}Pb/^{204}Pb$ (from Figure 5a)	≈19.8 ± 2.5	19.00 ± 0.63	19.91 ± 0.73	18.95 ± 0.68
$^{206}Pb/^{204}Pb$ (from Figure 5b)	≈20.4 ± 1.8	19.06 ± 0.19	19.68 ± 0.22	18.6 ± 1.1
$(Sr/Pb_{depl})/(Sr/Pb_{enrich})$	≈20		2.5 (max 33; min 0.18)	
$(Nd/Pb_{depl})/(Nd/Pb_{enrich})$	≈20		2.6 (max 9.1; min 0.096)	

with Nd isotopic compositions (see Figure 3 where data for *Ua Huka* define a trend that is indistinguishable from the field defined by the *Fatu Hiva group* islands – Tahuata, Fatu Hiva and Motane). This suggests that the process that created the Sr-Nd isotopic difference between the two groups did not decouple the Hf and Nd isotopic systems. Indeed, if Sr isotopes are plotted as a function of Hf isotopic compositions, the distinction highlighted in Figure 4 is reproduced. Finally, in Pb isotopic spaces, straight lines such as those reported for Hawaiian rocks are absent when all published data are compiled (Figures 3b and 3d). However, when only our high-precision Pb data are used, two trends with significantly different slopes can be distinguished (Figure 8). In each group, samples with high $^{206}Pb/^{204}Pb$ also have high $^{208}Pb/^{204}Pb$ but, for $^{207}Pb/^{204}Pb$, the arrays differ significantly since the slope of the *Ua Huka group* is positive while that of the *Fatu Hiva group* is slightly negative. In addition, the two arrays intersect at a $^{206}Pb/^{204}Pb$ of about 19.15. When $^{206}Pb/^{204}Pb$ is plotted versus $^{87}Sr/^{86}Sr$ or $^{143}Nd/^{144}Nd$ and all data from the literature are used, the two groups are also distinct: the *Fatu Hiva group* is always located at higher $^{206}Pb/^{204}Pb$ than the *Ua Huka group* (Figures 5a and 5b). The array defined by the *Fatu Hiva group* has a strong curvature that constrains the composition of two end-members, if interpreted as a mixing array. The enriched end-member (D) with elevated $^{87}Sr/^{86}Sr$ has a $^{206}Pb/^{204}Pb$ of 18.95 ± 0.68 while the depleted end-member (C) with low $^{87}Sr/^{86}Sr$ has a $^{206}Pb/^{204}Pb$ of 19.91 ± 0.73 (Table 3). Using the relationship between $^{143}Nd/^{144}Nd$ and $^{206}Pb/^{204}Pb$ ratios (see Figure 5b), we obtain similar values for the Pb isotopic compositions of the two end-members (C) and (D). Interestingly, the $^{206}Pb/^{204}Pb$ ratio close to 20 obtained for the depleted end-member of the *Fatu Hiva group* eliminates the possibility that this component is ambient depleted mantle, as sampled along mid-ocean ridges. We suggest therefore that the entire isotopic range defined by the lavas comes from isotopic heterogeneities located in the plume itself.

[25] In contrast to the *Fatu Hiva group*, the *Ua Huka group* defines far more diffuse arrays in Figures 5a and 5b suggesting that the isotopic heterogeneities cannot be simply explained by binary mixing when Pb isotopic compositions are considered. Nevertheless the mixing arrays point to a poorly defined $^{206}Pb/^{204}Pb$ ratio higher than 19.5

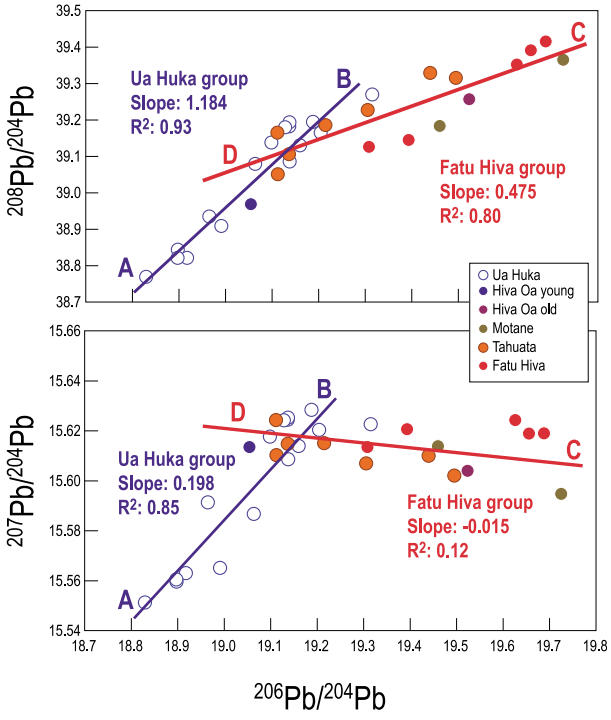

Figure 8. $^{208}Pb/^{204}Pb$ and $^{207}Pb/^{204}Pb$ versus $^{206}Pb/^{204}Pb$ for our Marquesas samples alone. The two groups define different slopes in both panels. The correlation coefficients R^2 are also shown. Letters A, B, C and D correspond to the potential four end-members defined in Figure 4.

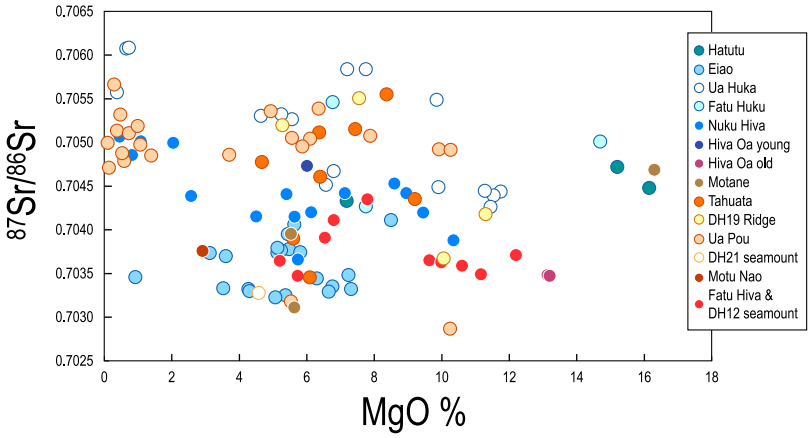

Figure 9. $^{87}Sr/^{86}Sr$ versus MgO showing the absence of negative correlation between the two parameters. Data from this study and GEOROC database.

for the depleted end-member (A) and the enriched end-member (B) has a better constrained $^{206}Pb/^{204}Pb$ ratio at 19.00 ± 0.63 (Table 3).

[26] The $^{206}Pb/^{204}Pb$ ratio of about 19 for the two enriched end-members (B and D) calculated using the observed correlations with Sr and Nd isotopic compositions in Figure 5 are entirely consistent with the tendencies shown by Pb isotopes measured on our samples alone (Figure 8). However, it is not the case for the depleted end-member of the *Ua Huka group* (end-member A), which has a value lower than 18.8 when our samples are considered alone (Figure 8) while it has a very poorly constrained value, but higher than 19.5, when all data are used (Figure 5). Acquisition of high-precision Pb isotopic data on samples from Eiao and Nuku Hiva might help solve the discrepancy.

[27] Finally, the curvature of the arrays in Figures 5a and 5b constrains the difference in Nd/Pb and Sr/Pb elemental ratios of the depleted and enriched components: for the *Fatu Hiva group*, the depleted end-member, which has high $^{206}Pb/^{204}Pb$, has Sr/Pb and Nd/Pb ratios that are about 2.5 times those of the enriched end-member (Table 3). For the *Ua Huka group*, the contrast between the two end-members is less well constrained but the relationships between $^{87}Sr/^{86}Sr$, $^{143}Nd/^{144}Nd$ and $^{206}Pb/^{204}Pb$ suggest that both Sr/Pb and Nd/Pb in the depleted component are significantly higher than in the enriched component (Table 3).

[28] Such differences in Sr/Pb and Nd/Pb ratios between sources should translate into differences in the lavas themselves and this is indeed seen when Sr/Pb and Nd/Pb are plotted as a function of $^{87}Sr/^{86}Sr$ (Figure S2) even though melting and fractional crystallization blurred the source ratios due to the difference in incompatibility of the three elements.

5.3. Origin of the Isotopic Stripes

[29] Since the two isotopic arrays are evident in small geographical areas (about 120 km for the Ua Huka trend and 60 km for the Fatu Hiva trend, see Figure 1) and located very close to one another in the archipelago, it is possible that the two trends originate through shallow processes. Contamination of the ascending magmas by the oceanic plate and overlying sediments could be a cause of isotopic changes, especially in the intermediate and evolved liquids [*Caroff et al.*, 1995, 1999; *Legendre et al.*, 2005a, 2005b]. In Figure 9, we demonstrate that the very large range of Sr isotopic compositions (0.7028 to 0.7061) is unrelated to the amount of MgO, a good proxy for fractional crystallization and potential interactions with the surrounding crust. We are therefore convinced that the range of isotopic compositions displayed by the Marquesas volcanics is not due to near-surface processes but is characteristic of the plume source.

[30] *Abouchami et al.* [2005] attributed the existence of the two Pb isotopic stripes in Hawaii to heterogeneities in the Hawaiian plume. More recently, the observation was extended to other isotopic systems and back in time to about 5 Ma [*Tanaka et al.*, 2008; *Weis*, 2010] but the origin of the asymmetry remains strongly debated. Very recently, *Weis* [2010] and *Weis et al.* [2011] associated the existence of the two Hawaiian trends with material from the Pacific "Large Low Shear Velocity Province" (LLSVP) located at the core-mantle boundary. They further

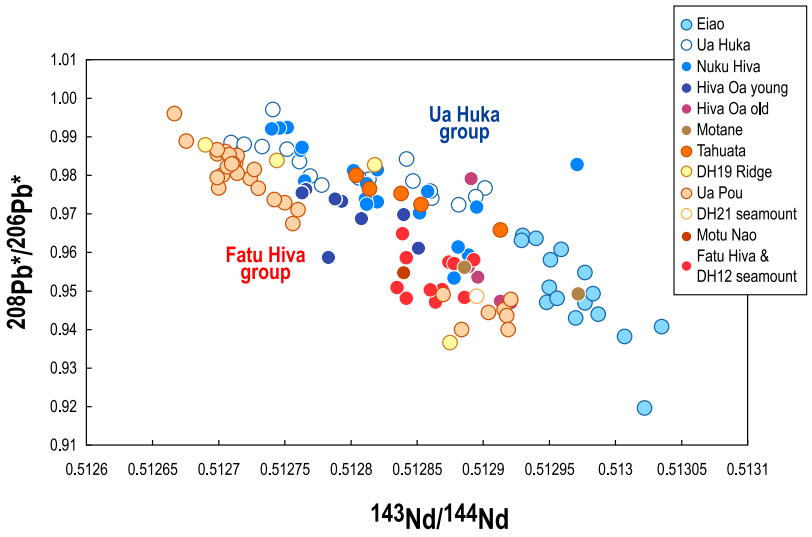

Figure 10. $^{208}Pb^*/^{206}Pb^*$ versus $^{143}Nd/^{144}Nd$ showing the same two parallel lines as in Sr versus Nd isotopic space. The two groups have similar $^{208}Pb^*/^{206}Pb^*$ in contrast to what has been observed in Hawaii [*Abouchami et al.*, 2005; *Weis*, 2010; *Huang et al.*, 2011; *Weis et al.*, 2011].

suggested that the isotopic similarities between Hawaii and Pitcairn were not fortuitous and that the two plumes were sampling the same source material. *Huang et al.* [2011] made a different parallel: they compared the Hawaiian isotopic stripes with similar features along Samoan and Marquesas islands to conclude that Hawaii was sampling the northern side of the Pacific LLSVP while Samoa and Marquesas were sampling its southern side. Like *Huang et al.* [2011], it might be argued that the location of the Marquesas Archipelago above the LLSVP could explain the two isotopic bands.

[31] Here we adopt a different approach because we believe that the main characteristics of the Marquesas isotopic stripes differ from those recognized for Hawaii and Samoa. We need to explain the coexistence of two different sources that melted next to each other below the Marquesas Archipelago for an extended period of time of over 5 Ma. First of all, in contrast to the sharp distinction in $^{208}Pb^*/^{206}Pb^*$ versus $^{143}Nd/^{144}Nd$ displayed by the Kea and Loa trends in Hawaii [*Huang et al.*, 2011; *Weis et al.*, 2011] and the Malu and Via trends in Samoa [*Huang et al.*, 2011], there is no significant difference in $^{208}Pb^*/^{206}Pb^*$ between the *Ua Huka* and the *Fatu Hiva* groups in the Marquesas (Figure 10). Indeed, the ranges of $^{208}Pb^*/^{206}Pb^*$ in the two groups are basically identical and the small difference seen in Figure 10 comes from the slightly higher $^{143}Nd/^{144}Nd$ ratios of the *Ua Huka group.* The real distinction between the two Marquesas groups comes primarily from the relationship between Nd and Sr isotopic compositions, as shown in Figure 4. The second very important difference is the strength and persistence of the plumes. The Hawaiian plume has been active for at least 85/81 Ma [*Regelous et al.*, 2003] and led to the production of very large volumes of lavas. Within the past million years, 213,000 km^3 of lavas erupted to form the Big Island of Hawaii [*Robinson and Eakins*, 2006], a figure that can be compared to the 42,500 km^3 of lavas produced over 5.5 Ma, the total length of volcanic activity documented in the Marquesas. In other words, while Hawaii results from the activity of a strong and long-lived plume that probably came from very deep in the mantle [*Sleep*, 1990], the Marquesas Archipelago results from a short-lived and weak plume. We believe the same model cannot apply to these two very different island chains.

[32] Many authors relate the superswell below French Polynesia, together with its numerous hot spots, to a very large thermochemical dome in the lower mantle. *Cadio et al.* [2011] proposed that this rising structure culminated at about 670 km depth and several little plumelets originated from this large hot plume. This structure is entirely consistent with *Courtillot et al.* [2003] who relate French Polynesia to "secondary plumes" from a large structure at the base of the upper mantle. We believe for the following reasons that this model is the most consistent with the geochemistry and age pattern of French Polynesia. The Polynesian island chains are numerous (Austral-Cook, Society, Marquesas and Pitcairn-

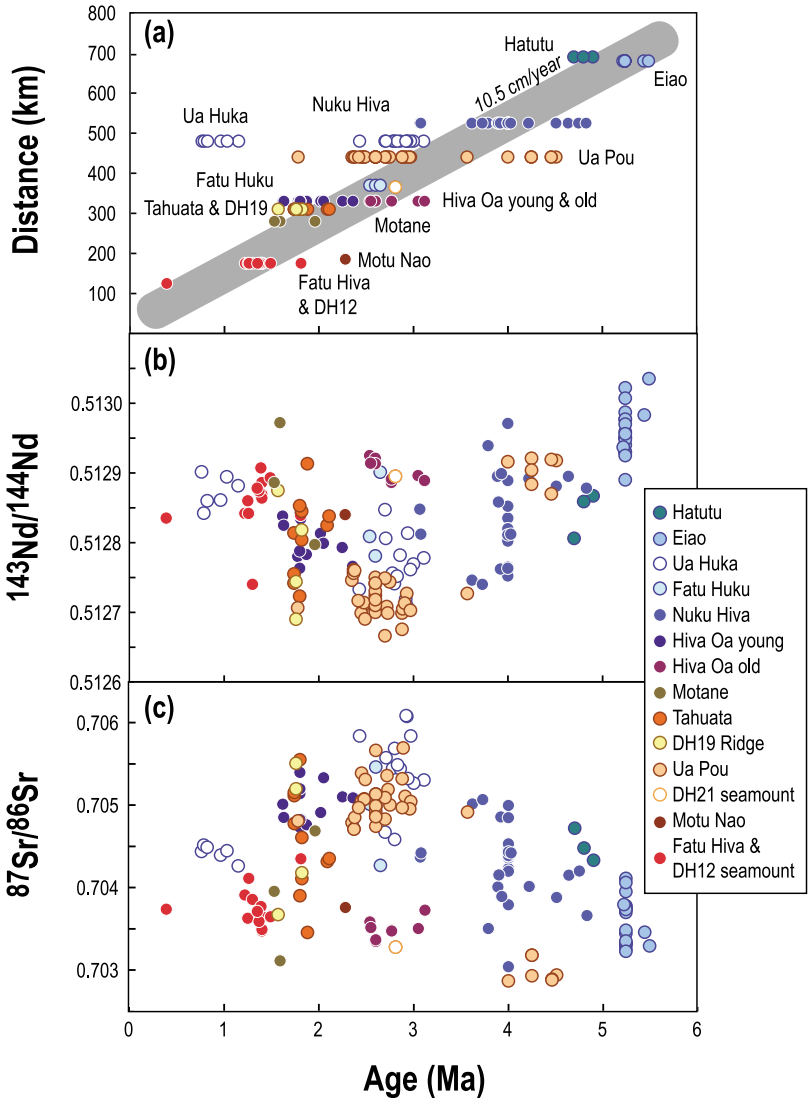

Figure 11. Age versus (a) distance, (b) $^{143}Nd/^{144}Nd$, and (c) $^{87}Sr/^{86}Sr$ showing that volcanism occurs with very different isotopic compositions in different locations at the same time. The distances are calculated along a N65°W direction with the zero point located on the MFZ Ridge. The gray field in Figure 11a corresponds to the Pacific plate motion. Geochemical data from this study and GEOROC database. The ages used here include values measured over 15 years ago on whole rocks [*Brousse et al.*, 1990; *Diraison*, 1991; *Le Dez*, 1996] and unfortunately, these data are probably not as accurate as those acquired more recently on groundmass (see Table S1).

Gambier) but restricted to a small geographical area (3.6 10^6 km^2), a tricky issue if plumes come from very deep in the mantle. In addition, the age pattern is also extremely complex with, for example, concomitant volcanic activity in three different locations in the Austral-Cook chain [*Turner and Jarrard*, 1982; *Chauvel et al.*, 1997] and near-synchronous eruptions over 300 km apart not only in the Marquesas (e.g., Ua Huka and Fatu Hiva; see Figure 11a) but also in the Austral-Cook chain [*Chauvel et al.*, 1997]. Moreover, the total volume of erupted lavas is very low (7,700 km^3 per Ma in the Marquesas, 11,000 km^3 per Ma in the Society, 6,600 km^3 per Ma in the Austral-Cook and only 3,000 km^3 per Ma in the Pitcairn-Gambier chain), a feature consistent with weak hot spots. In Polynesia, alkali basalts and basanites are extremely common and dominate over tholeiites, which suggests low-degree partial melting [*Caroff et al.*, 1997]. Finally, the sources are extremely heterogeneous, as shown by the large range of isotopic compositions. It is in this context that the two isotopic stripes in the Marquesas Archipelago must be examined. We believe that the very large isotopic range of each Marquesas island group originates from very low degree melts of an extremely heterogeneous plume. Small plumelets

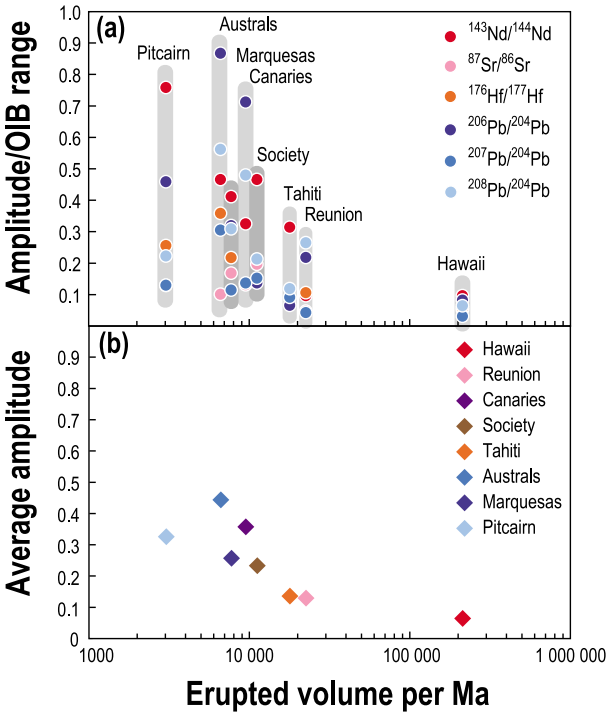

Figure 12. Amplitude of the isotopic variations relative to the entire range known for OIB plotted as a function of erupted volumes per Ma. (a) The amplitude for individual isotopic ratios and (b) the average value for the 6 isotopic ratios. Data are plotted for the Marquesas (this paper and data from GEOROC database), Austral-Cook, Pitcairn-Gambier, Society, Tahiti, Canary, Réunion and Hawaii (data from GEOROC database). Erupted volumes per Ma are calculated by dividing the estimated total volume of the island or archipelago (above the oceanic crust basement, see footnote of Table 2) by the time span between oldest and youngest ages. These volumes and times are 42,500 km^3 and 5.5 Ma for the Marquesas (Table 2); 50,300 km^3 (GMT, above the −3500 m isobaths) and 4.5 Ma [*Guillou et al.*, 2005] for Society including 25,000 km^3 and 1.4 Ma [*Hildenbrand et al.*, 2004] for Tahiti Island; 35,800 km^3 (GMT, above the −3,800 m isobath) and 11.8 Ma [*Guillou et al.*, 1994] for the Pitcairn-Gambier-Mururoa chain; 126,000 km^3 (GMT, above the −4000 m isobath) and 19 Ma [*Turner and Jarrard*, 1982] for the Austral-Cook; 195,800 km^3 [*Paris*, 2002] and 20.6 Ma [*Carracedo et al.*, 1998] for the Canary Islands; 85,000 km^3 (average value estimated from *Lénat et al.* [2001]) and 2.1 Ma [*Bosch et al.*, 2008] for Réunion Island; 213,000 km^3 [*Robinson and Eakins*, 2006] and 1.0 Ma [*Fekiacova et al.*, 2007; *Farnetani and Hofmann*, 2010] for Big Island, Hawaii.

from a large dome at the base of the upper mantle, as suggested by *Courtillot et al.* [2003] and *Cadio et al.* [2011], would sporadically ascend through the asthenosphere, each carrying the geochemical diversity of its source. Such activity explains why volcanism occurs at the same time in several locations (see Figure 11a) in the Marquesas Archipelago and why isotopically distinct magmas erupt synchronously within short distances (see for example, Ua Huka, Ua Pou, Fatu Huku and Hiva Oa between 2.5 and 3 Ma in Figures 11b and 11c).

5.4. Isotopic Heterogeneities and Plume Strength

[33] One of the most puzzling features of Polynesia is its remarkable isotopic heterogeneity: almost the entire range of Sr, Nd, Hf and Pb isotopic compositions known in ocean island basalts exists within the four island chains – Austral-Cook, Society, Pitcairn-Gambier and Marquesas (Figure 3). The question to be asked is how small islands, dispersed over a large area, can come from such diverse sources? Here we suggest that the range of isotopic heterogeneity is related to the strength of the plume. In Figure 12, we plot the isotopic variability of the island chains as a function of the volume of erupted lavas normalized per Ma of volcanic activity. The amplitude of change of Sr, Nd, Hf and the three Pb isotopic ratios for each island chain is normalized to the total range reported for OIB in the literature. To calculate the amplitude, we used data from this study and the GEOROC database and estimated the range simply by calculating the difference between the highest and the lowest values for each isotopic system. We believe that this is better than calculating averages and standard deviations because histograms of measured values do not define Gaussian curves with normal distributions. To calculate the volume of magmas erupted per Ma, we used literature data for the size of the islands or chains (sum of the emerged and immerged parts) and divided the total volume by the known duration of volcanic activity. This method overestimates the volumes emitted per Ma, as only the uppermost 3% to 10% of each edifice is generally sampled (during fieldwork on the islands, dredging or drilling) and dated, but it allows comparison between islands and linear chains. When volumes of volcanic edifices (islands and seamounts) were not available, we calculated them using GMT software and a reference isobath corresponding to the top of the oceanic crust in the bathymetric chart [*Smith and Sandwell*, 1997]. Further details including data and references for each island or island chain, are provided in Table 2 and in the caption of Figure 12.

[34] Figure 12 shows a negative correlation between the volume of lava emitted per Ma and the range of

isotopic compositions. Unfortunately, we could only plot few islands or island chains because of the limited set of available volumes for volcanic edifices. The Big Island of Hawaii, with its huge volcanic activity, has the smallest range, with normalized amplitude values below 0.2 while the Pitcairn-Gambier and Austral-Cook chains in Polynesia have the lowest magma productions and the largest amplitudes, up to almost 1 for $^{207}Pb/^{204}Pb$. Both the Marquesas and Society chains have low magma productions and high amplitudes. Interestingly, the six isotopic ratios considered here do not vary similarly in all island chains. Pb isotopes are the most variable in lavas of Reunion Island and the Austral-Cook and Canary chains where HIMU sources were identified. In contrast, Nd and Sr are the most variable in Pitcairn-Gambier, Marquesas, Societies and Hawaii as can be expected of magmas from enriched EM-type sources. Where data are available, the Hf isotopic compositions are almost always the least variable of all isotopic systems but this could be due to the much smaller data set for this isotopic system. Finally, the relative variability of the six isotopic systems not only demonstrates the complex nature of the plume sources but also demonstrates that when extreme compositions such as HIMU, EM I or EM II are present in an island chain, they usually coexist with very different compositions to produce the large observed variability. In contrast, where magma volumes are large, the isotopic variability is small. This suggests that the degree of partial melting controls the isotopic variability, an observation consistent with suggestions made by *Chabaux and Allègre* [1994] using U-Th-Ra disequilibria data. When the degree of melting is low, the source heterogeneity is transmitted to the lavas. In contrast, when high-degree melting leads to a large amount of magma, the source volume is larger, the heterogeneities are better mixed, and the diversity is blurred. In other words, small and isotopically heterogeneous islands such as the Marquesas, the Austral-Cook and Pitcairn-Gambier map the diversity of source compositions whereas large and isotopically more homogeneous islands such as Big Island (Hawaii) and Réunion Island are ideal sites to estimate the average composition of a plume source.

[35] In a way, what we suggest here for ocean islands extends the observation made about the diversity of isotopic compositions in melt inclusions. Authors such as *Saal et al.* [1998, 2005], *Jackson and Hart* [2006], *Paul et al.* [2011] or *Sobolev et al.* [2011] demonstrated that the isotopic variability in melt inclusions from oceanic island magmas was much larger than in the lavas themselves and they attributed the isotopic diversity to small scale sampling of the source material. In contrast, at the scale sampled by mid-ocean ridge basalts or ocean island basalts, most authors suggest that the observed isotopic diversity results from melting of a heterogeneous source in which low degree melts preferentially sample the enriched material, while higher melting degrees dilute this enriched material with larger proportions of more "normal" mantle [*Niu et al.*, 2002; *Donnelly et al.*, 2004; *Castillo et al.*, 2010; *Haase et al.*, 2011]. Using petrological arguments instead of isotopic constraints, *Sobolev et al.* [2005, 2007] also suggested that low-degree melts sampled fertile pyroxenite while the signature of the peridotitic source swamped high-degree melts. This model has become popular and today, many studies propose that mixing of isotopically enriched pyroxenitic melts with depleted peridotite melts explains magma compositions [*Jackson and Dasgupta*, 2008; *Day et al.*, 2009; *Dasgupta et al.*, 2010; *White*, 2010; *Day and Hilton*, 2011; *Gurenko et al.*, 2011; *Herzberg*, 2011; *Shorttle and Maclennan*, 2011]. Here, we extend this model and propose that ocean island lavas produced by low degree melts sample the isotopic diversity of their source area.

[36] The relationship between isotopic variability and magma production rate shown in Figure 12 can be used to constrain the size of heterogeneities in the plume source. We focus on the Marquesas Archipelago where we have abundant and precise isotopic data from accurately dated lavas. Our data from Ua Huka, Fatu Hiva and Tahuata show clearly that lavas erupted within <50,000 years have diverse isotopic compositions (e.g., UH34 and UH40 in Ua Huka, FH01 and FH18 in Fatu Hiva and TH05 and TH08 in Tahuata, Table 1). This suggests that the source that melted within this very short time interval was isotopically heterogeneous. Using the overall magma production rate of 42,500 km^3 over the 5.5 Ma of volcanic activity in the Marquesas, we estimate an average magma production of ≈400 km^3 in 50,000 years. Given the large proportion of basanites and alkali basalts in the Marquesas, we also estimate that the degree of partial melting is generally quite low, probably less than 5%. This indicates that over the period of 50,000 years, 400 km^3 of lava were produced from 8,000 km^3 of the mantle source. This small source volume can be represented as a sphere with a ca. 10 km radius. Such small-scale heterogeneity in a mantle plume is not surprising given the considerable

intraisland variations documented here as well as in previous studies of the Marquesas Archipelago.

6. Conclusions

[37] New isotopic (Sr, Nd, Pb, Hf) analyses of Marquesas lavas combined with literature data define two parallel rows of islands and seamounts with distinct and highly variable Nd and Sr isotopic compositions: the *Ua Huka group* in the northeast, and the *Fatu Hiva group* in the southwest. The two groups coexisted for the entire length of volcanic activity in the archipelago. The distinction between the two groups is less clear in other isotopic systems but in general the *Fatu Hiva group* has higher $^{206}Pb/^{204}Pb$ ratios than the *Ua Huka group* at any given $^{87}Sr/^{86}Sr$ value. Best fit hyperbolas for each island group demonstrate that the material that melted does not include ambient depleted mantle and was entirely contained in the plume source. The two end-members with depleted characteristics (low $^{87}Sr/^{86}Sr$ and high $^{143}Nd/^{144}Nd$) have $^{206}Pb/^{204}Pb$ ratios around 20 while the enriched end-members have more subdued values around 19. We attribute these isotopic stripes to melting of two adjacent filaments within the raising plume as suggested for Hawaii by *Farnetani and Hofmann* [2009, 2010].

[38] We suggest that the very large isotopic ranges of each Marquesas group originates from sampling by very low-degree melts of small portions (<10,000 km^3) of an extremely heterogeneous source in a large dome structure located under Polynesia. Similarly, the other Polynesian chains (Pitcairn-Gambier, Austral-Cook, Society) represent small volumes of magmas with unusually large isotopic variability. The same melting mechanism of other parts of the same dome could explain them as well. The contrast between the large isotopic variability observed in the surface expression of weak plumes (Polynesia) and the relative isotopic homogeneity of islands derived from strong plumes such as Hawaii or Réunion Island suggests that the factor controlling isotopic variability is the degree of partial melting. When partial melting degree is very low, source heterogeneity is preserved. In contrast, when high degrees of partial melting lead to high magma production rate, the diversity is blurred.

Acknowledgments

[39] We dedicate this study to the memory of Robert Brousse (1929–2010), pioneer of geological and petrologic studies in French Polynesia. He provided several samples used in this work, especially from Hiva Oa. Help from Sarah Bureau, Philippe Telouk and Philippe Nonnotte during analytical work was greatly appreciated. We thank Dominique Weis, an anonymous reviewer and the editor Joel Baker for their very constructive comments that helped us improve the overall content of the manuscript. This study was funded by CNRS (INSU and UMR 5025, 5275, 6538, 6518, 1572), BRGM, CEA-DASE and the ANR project "M &Ms."

References

Abouchami, W., A. W. Hofmann, S. J. G. Galer, F. A. Frey, J. Eisele, and M. D. Feigenson (2005), Lead isotopes reveal bilateral asymmetry and vertical continuity in the Hawaiian mantle plume, *Nature*, *434*, 851–856, doi:10.1038/nature03402.

Beccaluva, L., G. Bianchini, C. Natali, and F. Siena (2009), Continental flood basalts and mantle plumes: A case study of the northern Ethiopian Plateau, *J. Petrol.*, *50*(7), 1377–1403, doi:10.1093/petrology/egp024.

Blais, S., C. Legendre, R. C. Maury, G. Guille, H. Guillou, P. Rossi, and C. Chauvel (2008), Notice explicative, carte géologique de France, feuille de Ua Huka, Polynésie française, 102 pp., scale 1:30,000, Bur. de Rech. Géol. et Min., Orléans, France.

Blichert-Toft, J., and F. Albarède (2009), Mixing of isotopic heterogeneities in the Mauna Kea plume conduit, *Earth Planet. Sci. Lett.*, *282*(1–4), 190–200, doi:10.1016/j.epsl.2009.03.015.

Blichert-Toft, J., and W. M. White (2001), Hf isotope geochemistry of the Galapagos Islands, *Geochem. Geophys. Geosyst.*, *2*(9), 1043, doi:10.1029/2000GC000138.

Bosch, D., J. Blichert-Toft, F. Moynier, B. K. Nelson, P. Telouk, P. Y. Gillot, and F. Albarede (2008), Pb, Hf and Nd isotope compositions of the two Reunion volcanoes (Indian Ocean): A tale of two small-scale mantle "blobs"?, *Earth Planet. Sci. Lett.*, *265*(3–4), 748–765, doi:10.1016/j.epsl.2007.11.018.

Brousse, R., H. G. Barsczus, H. Bellon, J. M. Cantagrel, C. Diraison, H. Guillou, and C. Leotot (1990), The Marquesas alignment (French-Polynesia)—Volcanology, geochronology, a hot-spot model, *Bull. Soc. Geol. Fr.*, *6*(6), 933–949.

Cadio, C., I. Panet, A. Davaille, M. Diament, L. Métivier, and O. de Viron (2011), Pacific geoid anomalies revisited in light of thermochemical oscillating domes in the lower mantle, *Earth Planet. Sci. Lett.*, *306*(1–2), 123–135, doi:10.1016/j.epsl.2011.03.040.

Caress, D. V., M. K. McNutt, R. S. Detrick, and J. C. Mutter (1995), Seismic imaging of hotspot-related crustal underplating beneath the Marquesas Islands, *Nature*, *373*, 600–603, doi:10.1038/373600a0.

Caroff, M., R. C. Maury, P. Vidal, G. Guille, C. Dupuy, J. Cotten, H. Guillou, and P. Y. Gillot (1995), Rapid temporal changes in ocean island basalt composition—Evidence from an 800 m deep drill hole in Eiao shield (Marquesas), *J. Petrol.*, *36*(5), 1333–1365.

Caroff, M., R. C. Maury, G. Guille, and J. Cotten (1997), Partial melting below Tubuai (Austral Islands, French Polynesia), *Contrib. Mineral. Petrol.*, *127*, 369–382, doi:10.1007/s004100050286.

Caroff, M., H. Guillou, M. L. Lamiaux, R. C. Maury, G. Guille, and J. Cotten (1999), Assimilation of ocean crust by hawaiitic and mugearitic magmas: An example from Eiao (Marquesas), *Lithos*, *46*(2), 235–258, doi:10.1016/S0024-4937(98)00068-1.

Carracedo, J. C., S. Day, H. Guillou, E. R. Badiola, J. A. Canas, and F. J. P. Torrado (1998), Hotspot volcanism close to a passive continental margin: The Canary Islands, *Geol. Mag.*, *135*(5), 591–604, doi:10.1017/S0016756898001447.

Castillo, P. R., P. Scarsi, and H. Craig (2007), He, Sr, Nd, and Pb isotopic constraints on the origin of the Marquesas and other linear volcanic chains, *Chem. Geol.*, *240*(3–4), 205, doi:10.1016/j.chemgeo.2007.02.012.

Castillo, P. R., D. A. Clague, A. S. Davis, and P. F. Lonsdale (2010), Petrogenesis of Davidson Seamount lavas and its implications for fossil spreading center and intraplate magmatism in the eastern Pacific, *Geochem. Geophys. Geosyst.*, *11*, Q02005, doi:10.1029/2009GC002992.

Chabaux, F., and C. J. Allègre (1994), ^{238}U-^{230}Th-^{226}Ra disequilibria in volcanics: A new insight into melting conditions, *Earth Planet. Sci. Lett.*, *126*(1–3), 61–74, doi:10.1016/0012-821X(94)90242-9.

Charbit, S., H. Guillou, and L. Turpin (1998), Cross calibration of K-Ar standard minerals using an unspiked Ar measurement technique, *Chem. Geol.*, *150*(1–2), 147–159, doi:10.1016/S0009-2541(98)00049-7.

Chauvel, C., and J. Blichert-Toft (2001), A hafnium isotope and trace element perspective on melting of the depleted mantle, *Earth Planet. Sci. Lett.*, *190*, 137–151, doi:10.1016/S0012-821X(01)00379-X.

Chauvel, C., and C. Hémond (2000), Melting of a complete section of recycled oceanic crust: Trace element and Pb isotopic evidence from Iceland, *Geochem. Geophys. Geosyst.*, *1*(2), 1001, doi:10.1029/1999GC000002.

Chauvel, C., W. McDonough, G. Guille, R. Maury, and R. Duncan (1997), Contrasting old and young volcanism in Rurutu Island, Austral Chain, *Chem. Geol.*, *139*, 125–143, doi:10.1016/S0009-2541(97)00029-6.

Chauvel, C., S. Blais, R. Maury, and E. Lewin (2009), Isotopic streaks suggest a stripy plume under the Marquesas, *Eos Trans. AGU*, *90*(52), Fall Meet. Suppl., Abstract V24A-05.

Chauvel, C., S. Bureau, and C. Poggi (2011), Comprehensive chemical and isotopic analyses of basalt and sediment reference materials, *Geostand. Geoanal. Res.*, *35*(1), 125–143, doi:10.1111/j.1751-908X.2010.00086.x.

Cotten, J., A. Le Dez, M. Bau, M. Caroff, R. C. Maury, P. Dulski, S. Fourcade, M. Bohn, and R. Brousse (1995), Origin of anomalous rare-earth element and yttrium enrichments in subaerially exposed basalts: Evidence form French Polynesia, *Chem. Geol.*, *119*, 115–138, doi:10.1016/0009-2541(94)00102-E.

Courtillot, V., A. Davaille, J. Besse, and J. Stock (2003), Three distinct types of hotspots in the Earth's mantle, *Earth Planet. Sci. Lett.*, *205*(3–4), 295–308, doi:10.1016/S0012-821X(02)01048-8.

Crough, S. T., and R. D. Jarrard (1981), The Marquesas-line swell, *J. Geophys. Res.*, *86*(B12), 11,763–11,771, doi:10.1029/JB086iB12p11763.

Daoud, M. A., R. C. Maury, J. A. Barrat, R. N. Taylor, B. Le Gall, H. Guillou, J. Cotten, and J. Rolet (2010), A LREE-depleted component in the Afar plume: Further evidence from Quaternary Djibouti basalts, *Lithos*, *114*(3–4), 327–336, doi:10.1016/j.lithos.2009.09.008.

Dasgupta, R., M. G. Jackson, and C. T. A. Lee (2010), Major element chemistry of ocean island basalts—Conditions of mantle melting and heterogeneity of mantle source, *Earth Planet. Sci. Lett.*, *289*(3–4), 377–392, doi:10.1016/j.epsl.2009.11.027.

Davaille, A. (1999), Simultaneous generation of hotspots and superswells by convection in a heterogeneous planetary mantle, *Nature*, *402*, 756–760, doi:10.1038/45461.

Day, J. M. D., and D. R. Hilton (2011), Origin of ^{3}He/^{4}He ratios in HIMU-type basalts constrained from Canary Island lavas, *Earth Planet. Sci. Lett.*, *305*(1–2), 226–234, doi:10.1016/j.epsl.2011.03.006.

Day, J. M. D., D. G. Pearson, C. G. Macpherson, D. Lowry, and J. C. Carracedo (2009), Pyroxenite-rich mantle formed by recycled oceanic lithosphere: Oxygen-osmium isotope evidence from Canary Island lavas, *Geology*, *37*(6), 555–558, doi:10.1130/G25613A.1.

Desonie, D. L., R. A. Duncan, and J. H. Natland (1993), Temporal and geochemical variability of volcanic products of the Marquesas hotspot, *J. Geophys. Res.*, *98*(B10), 17,649–17,665, doi:10.1029/93JB01562.

Devey, C. W., and K. M. Haase (2003), The sources for hotspot volcanism in the South Pacific Ocean, in *Oceanic Hotspots: Intraplate Submarine Magmatism and Tectonism*, edited by P. S. R. Hékinian and J. L. Cheminée, pp. 253–284, Springer, Berlin, doi:10.1007/978-3-642-18782-7_9.

Diraison, C. (1991), Le volcanisme aérien des archipels polynésiens de la Société, des Marquises et des Australes-Cook. Téphrostratigraphie, datation isotopique et géochimie comparées. Contribution à l'étude des origines du volcanisme intraplaque du Pacifique central, PhD thesis, 413 pp., Univ. de Bretagne Occidentale, Brest, France.

Donnelly, K. E., S. L. Goldstein, C. H. Langmuir, and M. Spiegelman (2004), Origin of enriched ocean ridge basalts and implications for mantle dynamics, *Earth Planet. Sci. Lett.*, *226*(3–4), 347–366, doi:10.1016/j.epsl.2004.07.019.

Dostal, J., B. Cousens, and C. Dupuy (1998), The incompatible element characteristics of an ancient subducted sedimentary component in ocean island basalts from French Polynesia, *J. Petrol.*, *39*(5), 937–952, doi:10.1093/petroj/39.5.937.

Doucet, S., D. Weis, J. S. Scoates, K. N. Nicolaysen, F. H. Frey, and A. Giret (2002), Petrogenesis of high- and low-MgO transitional basalts from the Loranchet Peninsula (Mont des Ruches, Mont Fontaine), Kerguelen Archipelago, *J. Petrol.*, *43*, 1341–1366, doi:10.1093/petrology/43.7.1341.

Duncan, R. A., and I. McDougall (1974), Migration of volcanism with time in the Marquesas Islands, French Polynesia, *Earth Planet. Sci. Lett.*, *21*(4), 414–420, doi:10.1016/0012-821X(74)90181-2.

Duncan, R. A., M. T. McCulloch, H. G. Barczus, and D. R. Nelson (1986), Plume versus lithospheric sources for the melts at Ua Pou, Marquesas Island, *Nature*, *303*, 142–146.

Dupuy, C., P. Vidal, H. G. Barsczus, and C. Chauvel (1987), Origin of basalts from the Marquesas Archipelago (south central Pacific Ocean): Isotope and trace element constraints, *Earth Planet. Sci. Lett.*, *82*, 145–152, doi:10.1016/0012-821X(87)90114-2.

Farnetani, C. G., and A. W. Hofmann (2009), Dynamics and internal structure of a lower mantle plume conduit, *Earth Planet. Sci. Lett.*, *282*(1–4), 314–322, doi:10.1016/j.epsl.2009.03.035.

Farnetani, C. G., and A. W. Hofmann (2010), Dynamics and internal structure of the Hawaiian plume, *Earth Planet. Sci. Lett.*, *295*(1–2), 231–240, doi:10.1016/j.epsl.2010.04.005.

Fekiacova, Z., W. Abouchami, S. J. G. Galer, M. O. Garcia, and A. W. Hofmann (2007), Origin and temporal evolution of Ko'olau Volcano, Hawai'i: Inferences from isotope data on the Ko'olau Scientific Drilling Project (KSDP), the

Honolulu Volcanics and ODP Site 843, *Earth Planet. Sci. Lett.*, *261*(1–2), 65–83, doi:10.1016/j.epsl.2007.06.005.

Filmer, P. E., M. K. McNutt, and C. J. Wolfe (1993), Elastic thickness of the lithosphere in the Marquesas and Society Islands, *J. Geophys. Res.*, *98*(B11), 19,565–19,577, doi:10.1029/93JB01720.

Fitton, J. G., A. D. Saunders, P. D. Kempton, and B. S. Hardarson (2003), Does depleted mantle form an intrinsic part of the Iceland plume?, *Geochem. Geophys. Geosyst.*, *4*(3), 1032, doi:10.1029/2002GC000424.

Frey, F. A., S. Huang, J. Blichert-Toft, M. Regelous, and M. Boyet (2005), Origin of depleted components in basalt related to the Hawaiian hot spot: Evidence from isotopic and incompatible element ratios, *Geochem. Geophys. Geosyst.*, *6*, Q02L07, doi:10.1029/2004GC000757.

Furman, T., J. Bryce, T. Rooney, B. Hana, G. Yirgu, and D. Ayalew (2006), Heads and tails: 30 million years of the Afar plume, in *The Afar Volcanic Province Within the East African Rift System*, edited by G. Yirgu, C. J. Ebinger, and P. K. H. Maguire, *Geol. Soc. Spec. Publ.*, *259*, 95–119, doi:10.1144/GSL.SP.2006.259.01.09.

Galer, S. J. G., and W. Abouchami (1998), Practical application of lead triple spiking for correction of instrumental mass discrimination, *Mineral. Mag.*, *62A*, 491–492, doi:10.1180/minmag.1998.62A.1.260.

Garcia, M. O., L. Swinnard, D. Weis, A. R. Greene, T. Tagami, H. Sano, and C. E. Gandy (2010), Petrology, geochemistry and geochronology of Kaua'i lavas over 4.5 Myr: Implications for the origin of rejuvenated volcanism and the evolution of the Hawaiian plume, *J. Petrol.*, *51*, 1507–1540, doi:10.1093/petrology/egq027.

Guille, G., C. Legendre, R. C. Maury, M. Caroff, M. Munschy, S. Blais, C. Chauvel, J. Cotten, and H. Guillou (2002), Les Marquises (Polynésie française): Un archipel intraocéanique atypique, *Geol. Fr.*, *2*, 5–36.

Guillou, H., P.-Y. Gillot, and G. Guille (1994), Age (K-Ar) et position des îles Gambier dans l'alignement du point chaud de Pitcairn (Pacifique Sud), *C. R. Acad. Sci., Ser. II*, *318*, 635–641.

Guillou, H., R. C. Maury, S. Blais, J. Cotten, C. Legendre, G. Guille, and M. Caroff (2005), Age progression along the Society hotspot chain (French Polynesia) based on new unspiked K-Ar ages, *Bull. Soc. Geol. Fr.*, *176*(2), 135–150, doi:10.2113/176.2.135.

Guillou, H., S. Nomade, J. C. Carracedo, C. Kissel, C. Laj, F. J. Perez Torrado, and C. Wandres (2011), Effectiveness of combined unspiked K-Ar and $^{40}Ar/^{39}Ar$ dating methods in the ^{14}C age range, *Quat. Geochronol.*, *6*(6), 530–538, doi:10.1016/j.quageo.2011.03.011.

Gurenko, A. A., I. N. Bindeman, and M. Chaussidon (2011), Oxygen isotope heterogeneity of the mantle beneath the Canary Islands: Insights from olivine phenocrysts, *Contrib. Mineral. Petrol.*, *162*(2), 349–363, doi:10.1007/s00410-010-0600-5.

Gutscher, M. A., J. L. Olivet, D. Aslanian, J. P. Eissen, and R. Maury (1999), The "lost Inca Plateau": Cause of flat subduction beneath Peru?, *Earth Planet. Sci. Lett.*, *171*(3), 335–341, doi:10.1016/S0012-821X(99)00153-3.

Haase, K. M., M. Regelous, R. A. Duncan, P. A. Brandl, N. Stroncik, and I. Grevemeyer (2011), Insights into mantle composition and mantle melting beneath mid-ocean ridges from postspreading volcanism on the fossil Galapagos Rise, *Geochem. Geophys. Geosyst.*, *12*, Q0AC11, doi:10.1029/2010GC003482.

Hanano, D., D. Weis, J. S. Scoates, S. Aciego, and D. J. DePaolo (2010), Horizontal and vertical zoning of heterogeneities in the Hawaiian mantle plume from the geochemistry of consecutive postshield volcano pairs: Kohala-Mahukona and Mauna Kea–Hualalai, *Geochem. Geophys. Geosyst.*, *11*, Q01004, doi:10.1029/2009GC002782.

Hart, S. R. (1988), Heterogeneous mantle domains: Signatures, genesis and mixing chronologies, *Earth Planet. Sci. Lett.*, *90*, 273–296, doi:10.1016/0012-821X(88)90131-8.

Hart, S. R., E. H. Hauri, L. A. Oshmann, and J. A. Whitehead (1992), Mantle plumes and entrainment: Isotopic evidence, *Science*, *256*, 517–520, doi:10.1126/science.256.5056.517.

Herzberg, C. (2011), Identification of source lithology in the Hawaiian and Canary Islands: Implications for origins, *J. Petrol.*, *52*(1), 113–146, doi:10.1093/petrology/egq075.

Hildenbrand, A., P. Y. Gillot, and I. Le Roy (2004), Volcano-tectonic and geochemical evolution of an oceanic intra-plate volcano: Tahiti-Nui (French Polynesia), *Earth Planet. Sci. Lett.*, *217*(3–4), 349–365, doi:10.1016/S0012-821X(03)00599-5.

Hoernle, K., R. Werner, J. P. Morgan, D. Garbe-Schonberg, J. Bryce, and J. Mrazek (2000), Existence of complex spatial zonation in the Galapagos plume for at least 14 m.y., *Geology*, *28*(5), 435–438, doi:10.1130/0091-7613(2000)028<0435:EOCSZI>2.3.CO;2.

Hofmann, A. W., K. P. Jochum, M. Seufert, and W. M. White (1986), Nb and Pb in oceanic basalts: New constraints on mantle evolution, *Earth Planet. Sci. Lett.*, *79*, 33–45, doi:10.1016/0012-821X(86)90038-5.

Huang, S., P. S. Hall, and M. G. Jackson (2011), Geochemical zoning of volcanic chains associated with Pacific hotspots, *Nat. Geosci.*, *4*(12), 874–878, doi:10.1038/ngeo1263.

Jackson, M. G., and R. Dasgupta (2008), Compositions of HIMU, EM1, and EM2 from global trends between radiogenic isotopes and major elements in ocean island basalts, *Earth Planet. Sci. Lett.*, *276*(1–2), 175–186, doi:10.1016/j.epsl.2008.09.023.

Jackson, M. G., and S. R. Hart (2006), Strontium isotopes in melt inclusions from Samoan basalts: Implications for heterogeneity in the Samoan plume, *Earth Planet. Sci. Lett.*, *245*(1–2), 260–277, doi:10.1016/j.epsl.2006.02.040.

Jordahl, K. A., M. K. McNutt, H. F. Webb, S. E. Kruse, and M. G. Kuykendall (1995), Why there are no earthquakes on the Marquesas Fracture Zone, *J. Geophys. Res.*, *100*(B12), 24,431–24,447, doi:10.1029/94JB02886.

Kerr, A. C., A. D. Saunders, J. Tarney, N. H. Berry, and V. L. Hards (1995), Depleted mantle-plume geochemical signatures: No paradox for plume theories, *Geology*, *23*, 843–846, doi:10.1130/0091-7613(1995)023<0843:DMPGSN>2.3.CO;2.

Kokfelt, T. F., K. Hoernle, F. Hauff, J. Fiebig, R. Werner, and D. Garbe-Schonberg (2006), Combined trace element and Pb-Nd-Sr-O isotope evidence for recycled oceanic crust (upper and lower) in the Iceland mantle plume, *J. Petrol.*, *47*(9), 1705–1749, doi:10.1093/petrology/egl025.

Laughlin, A. W., J. Poths, H. A. Healey, S. Reneau, and G. Woldegabriel (1994), Dating of Quaternary basalts using the cosmogenic He-3 and C-14 methods with implications for excess Ar-40, *Geology*, *22*, 135–138, doi:10.1130/0091-7613(1994)022<0135:DOQBUT>2.3.CO;2.

Le Dez, A. (1996), Variations pétrologiques et géochimiques associées à l'édification des volcans-boucliers de Polynésie française: Exemples de Nuku Hiva et Hiva Oa (Marquises) et de Moorea (Société), PhD thesis, 407 pp., Univ. de Bretagne Occidentale, Brest, France.

Le Dez, A., R. C. Maury, P. Vidal, H. Bellon, J. Cotten, and R. Brousse (1996), Geology and geochemistry of Nuku Hiva, Marquesas: Temporal trends in a large Polynesian shield volcano, *Bull. Soc. Geol. Fr.*, *167*(2), 197–209.

Legendre, C., R. C. Maury, D. Savanier, J. Cotten, C. Chauvel, C. Hémond, C. Bollinger, G. Guille, S. Blais, and P. Rossi (2005a), The origin of intermediate and evolved lavas in the Marquesas archipelago: An example from Nuku Hiva island (French Polynesia), *J. Volcanol. Geotherm. Res.*, *143*, 293–317, doi:10.1016/j.jvolgeores.2004.12.001.

Legendre, C., et al. (2005b), Origin of exceptionally abundant phonolites on Ua Pou island (Marquesas, french Polynesia): Partial melting of basanites followed by crustal contamination, *J. Petrol.*, *46*, 1925–1962, doi:10.1093/petrology/egi043.

Legendre, C., R. C. Maury, S. Blais, H. Guillou, and J. Cotten (2006), Atypical hotspot chains: Evidence for a secondary melting zone below the Marquesas (French Polynesia), *Terra Nova*, *18*(3), 210–216, doi:10.1111/j.1365-3121.2006.00681.x.

Lénat, J. F., B. Gibert-Malengreau, and A. Galdeano (2001), A new model for the evolution of the volcanic island of Reunion (Indian Ocean), *J. Geophys. Res.*, *106*(B5), 8645–8663, doi:10.1029/2000JB900448.

Maury, R. C., G. Guille, C. Legendre, D. Savanier, H. Guillou, P. Rossi, and S. Blais (2006), Notice explicative, carte géologique de France, feuille de Nuku Hiva, Polynésie française, 116 pp., scale 1:50,000, Bur. de Rech. Géol. et Min., Orléans, France.

Maury, R. C., et al. (2012), Notice explicative, carte géologique de France, feuille de Hiva Oa–Tahuata–Motane et Fatu Hiva, scale 1:100,000, Bur. de Rech. Géol. et Min., Orléans, France, in press.

McDonough, W. F., and S. S. Sun (1995), The composition of the Earth, *Chem. Geol.*, *120*, 223–253, doi:10.1016/0009-2541(94)00140-4.

McNutt, M. K. (1998), Superswells, *Rev. Geophys.*, *36*(2), 211–244, doi:10.1029/98RG00255.

McNutt, M., and A. Bonneville (2000), A shallow, chemical origin for the Marquesas Swell, *Geochem. Geophys. Geosyst.*, *1*(6), 1014, doi:10.1029/1999GC000028.

McNutt, M., K. Fischer, S. Kruse, and J. Natland (1989), The origin of the Marquesas fracture-zone ridge and its implications for the nature of hot spots, *Earth Planet. Sci. Lett.*, *91*(3–4), 381–393, doi:10.1016/0012-821X(89)90012-5.

Montelli, R., G. Nolet, F. A. Dahlen, and G. Masters (2006), A catalogue of deep mantle plumes: New results from finite-frequency tomography, *Geochem. Geophys. Geosyst.*, *7*, Q11007, doi:10.1029/2006GC001248.

Niu, Y., M. Regelous, I. J. Wendt, R. Batiza, and M. J. O'Hara (2002), Geochemistry of near-EPR seamounts: Importance of source vs. process and the origin of enriched mantle component, *Earth Planet. Sci. Lett.*, *199*(3–4), 327–345, doi:10.1016/S0012-821X(02)00591-5.

Paris, R. (2002), Volcanic construction and destruction rates of hotspot islands: The Canary Islands example (Spain), PhD thesis, Univ. of Las Palmas, Las Palmas de Gran Canaria, Spain.

Paul, B., J. D. Woodhead, J. Hergt, L. Danyushevsky, T. Kunihiro, and E. Nakamura (2011), Melt inclusion Pb-isotope analysis by LA-MC-ICPMS: Assessment of analytical performance and application to OIB genesis, *Chem. Geol.*, *289*(3–4), 210–223, doi:10.1016/j.chemgeo.2011.08.005.

Pautot, G., and J. Dupont (1974), La zone de fracture des Marquises, *C. R. Acad. Sci. Paris*, *279*, 1519–1523.

Regelous, M., A. W. Hofmann, W. Abouchami, and S. J. G. Galer (2003), Geochemistry of lavas from the Emperor Seamounts, and the geochemical evolution of Hawaiian magmatism from 85 to 42 Ma, *J. Petrol.*, *44*(1), 113–140, doi:10.1093/petrology/44.1.113.

Robinson, J. E., and B. W. Eakins (2006), Calculated volumes of individual shield volcanoes at the young end of the Hawaiian Ridge, *J. Volcanol. Geotherm. Res.*, *151*(1–3), 309–317, doi:10.1016/j.jvolgeores.2005.07.033.

Romanowicz, B., and Y. Gung (2002), Superplumes from the core-mantle boundary to the lithosphere: Implications for heat flux, *Science*, *296*(5567), 513–516, doi:10.1126/science.1069404.

Saal, A. E., S. R. Hart, N. Shimizu, E. H. Hauri, and G. D. Layne (1998), Pb isotopic variability in melt inclusions from oceanic island basalts, Polynesia, *Science*, *282*, 1481–1484, doi:10.1126/science.282.5393.1481.

Saal, A. E., S. R. Hart, N. Shimizu, E. H. Hauri, G. D. Layne, and J. M. Eiler (2005), Pb isotopic variability in melt inclusions from the EMI-EMII-HIMU mantle end-members and the role of the oceanic lithosphere, *Earth Planet. Sci. Lett.*, *240*, 605–620, doi:10.1016/j.epsl.2005.10.002.

Saal, A. E., M. D. Kurz, S. R. Hart, J. S. Blusztajn, J. Blichert-Toft, Y. Liang, and D. J. Geist (2007), The role of lithospheric gabbros on the composition of Galapagos lavas, *Earth Planet. Sci. Lett.*, *257*(3–4), 391–406, doi:10.1016/j.epsl.2007.02.040.

Saunders, A. D., M. Storey, R. W. Kent, and M. J. Norry (1992), Consequences of plume-lithosphere interactions, in *Magmatism and the Causes of Continental Break-Up*, edited by B. C. Storey, T. Alabaster, and R. J. Pankhurst, *Geol. Soc. Spec. Publ.*, *68*, 41–60.

Shorttle, O., and J. Maclennan (2011), Compositional trends of Icelandic basalts: Implications for short–length scale lithological heterogeneity in mantle plumes, *Geochem. Geophys. Geosyst.*, *12*, Q11008, doi:10.1029/2011GC003748.

Sleep, N. H. (1990), Hotspot and mantle plumes: Some phenomenology, *J. Geophys. Res.*, *95*, 6715–6736, doi:10.1029/JB095iB05p06715.

Smith, W. H. F., and D. T. Sandwell (1997), Global sea floor topography from satellite altimetry and ship depth soundings, *Science*, *277*(5334), 1956–1962, doi:10.1126/science.277.5334.1956.

Sobolev, A. V., A. W. Hofmann, S. V. Sobolev, and I. K. Nikogosian (2005), An olivine-free mantle source of Hawaiian shield basalts, *Nature*, *434*(7033), 590–597, doi:10.1038/nature03411.

Sobolev, A. V., et al. (2007), The amount of recycled crust in sources of mantle-derived melts, *Science*, *316*(5823), 412–417, doi:10.1126/science. 1138113.

Sobolev, A. V., A. W. Hofmann, K. P. Jochum, D. V. Kuzmin, and B. Stoll (2011), A young source for the Hawaiian plume, *Nature*, *476*(7361), 434–437, doi:10.1038/nature10321.

Steiger, R. H., and E. Jäger (1977), Subcommission on geochronology: Convention on the use of decay constants in geo-and cosmochronology, *Earth Planet. Sci. Lett.*, *36*, 359–362, doi:10.1016/0012-821X(77)90060-7.

Tanaka, R., A. Makishima, and E. Nakamura (2008), Hawaiian double volcanic chain triggered by an episodic involvement of recycled material: Constraints from temporal Sr-Nd-Hf-Pb isotopic trend of the Loa-type volcanoes, *Earth Planet. Sci. Lett.*, *265*(3–4), 450–465, doi:10.1016/j.epsl.2007.10.035.

Tatsumoto, M. (1978), Isotopic composition of lead in oceanic basalts and its implication to mantle evolution, *Earth Planet. Sci. Lett.*, *38*, 63–87, doi:10.1016/0012-821X(78)90126-7.

Thirlwall, M. F., M. A. M. Gee, R. N. Taylor, and B. J. Murton (2004), Mantle components in Iceland and adjacent ridges investigated using double-spike Pb isotope ratios, *Geochim. Cosmochim. Acta*, *68*(2), 361–386, doi:10.1016/S0016-7037(03)00424-1.

Turner, D. L., and R. D. Jarrard (1982), K-Ar dating of the Cook-Austral chain: A test of the hot-spot hypothesis, *J. Volcanol. Geotherm. Res.*, *12*, 187–220, doi:10.1016/0377-0273(82)90027-0.

Vidal, P., C. Chauvel, and R. Brousse (1984), Large mantle heterogeneity beneath French Polynesia, *Nature*, *307*, 536–538, doi:10.1038/307536a0.

Vidal, P., C. Dupuy, H. G. Barsczus, and C. Chauvel (1987), Hétérogénéités du manteau et origine des basaltes des Marquises (Polynésie), *Bull. Soc. Geol. Fr.*, *4*, 633–642.

Weis, D. (2010), Daly lecture: Geochemical insights into mantle geodynamics and plume structure, Abstract V41F-01 presented at 2010 Fall Meeting, AGU, San Francisco, Calif.

Weis, D., M. O. Garcia, J. M. Rhodes, M. Jellinek, and J. S. Scoates (2011), Role of the deep mantle in generating the compositional asymmetry of the Hawaiian mantle plume, *Nat. Geosci.*, *4*(12), 831–838, doi:10.1038/ngeo1328.

White, W. M. (2010), Oceanic island basalts and mantle plumes: The geochemical perspective, *Annu. Rev. Earth Planet. Sci.*, *38*, 133–160, doi:10.1146/annurev-earth-040809-152450.

White, W. M., A. R. McBirney, and R. A. Duncan (1993), Petrology and geochemistry of the Galapagos Islands: Portrait of a pathological mantle plume, *J. Geophys. Res.*, *98*(B11), 19,533–19,563, doi:10.1029/93JB02018.

White, W. M., F. Albarède, and P. Télouk (2000), High-precision analysis of Pb isotope ratios by multi-collector ICP-MS, *Chem. Geol.*, *167*, 257–270, doi:10.1016/S0009-2541(99)00182-5.

Willbold, M., and A. Stracke (2006), Trace element composition of mantle end-members: Implications for recycling of oceanic and upper and lower continental crust, *Geochem. Geophys. Geosyst.*, *7*, Q04004, doi:10.1029/2005GC001005.

Woodhead, J. D. (1992), Temporal geochemical evolution in oceanic intra-plate volcanics: A case study from the Marquesas (French Polynesia) and comparison with other hotspots, *Contrib. Mineral. Petrol.*, *111*, 458–467, doi:10.1007/BF00320901.

Yang, H. J., F. A. Frey, and D. A. Clague (2003), Constraints on the source components of lavas forming the Hawaiian North Arch and Honolulu volcanics, *J. Petrol.*, *44*(4), 603–627, doi:10.1093/petrology/44.4.603.